Geogr. Fis. Dinam. Quat.
40 (2017). 137-159

DOI 10.4461/GFDQ.2017.40.10

ALEXANDER R. GROOS [1*], CHRISTOPH MAYER [2], CLAUDIO SMIRAGLIA [3],
GUGLIELMINA DIOLAIUTI [3], ASTRID LAMBRECHT [2]

A FIRST ATTEMPT TO MODEL REGION-WIDE GLACIER SURFACE MASS BALANCES IN THE KARAKORAM: FINDINGS AND FUTURE CHALLENGES

ABSTRACT: GROOS A.R., MAYER C., SMIRAGLIA C., DIOLAIUTI G., LAMBRECHT A., *A first attempt to model region-wide glacier surface mass balances in the Karakoram: findings and future challenges.* (IT ISSN 0391-9838, 2017).

In contrast to the central and eastern part of High Mountain Asia (HMA), no extensive glacier mass loss has been observed in the Karakoram during previous decades. However, the potential meteorological and glaciological causes of the so-called Karakoram Anomaly are diverse and still under debate. This paper introduces and presents a novel glacier Surface Mass Balance Model (glacierSMBM) to test whether the characteristic regional mass balance pattern can be reproduced using recent field, remote-sensing and reanalysis data as input. A major advantage of the model setup is the implementation of the non-linear effect of supra-glacial debris on the sub-surface ice melt. In addition to a first assessment of the annual surface mass balance from 1st August 2010 until 31st July 2011, a sensitivity analysis was performed to investigate the response of Karakoram glaciers to recent climate change. The mean modelled glacier mass balance for the Karakoram during the observation period is -0.92 m water equivalent (w.e.) a^{-1} and corresponds to an annual melt water contribution of ~12.66 km^3. Data inaccuracies and the neglected process of snow redistribution from adjacent slopes are probably responsible for the bias in the model output. Despite the general offset between mass gain and mass loss, the model captures the characteristic features of the anomaly and indicates that positive glacier mass balances are mainly restricted to the central and northeastern part of the mountain range. From the evaluation of the sensitivity analysis, it can be concluded that the complex glacier response in the Karakoram is not the result of a single driver, but related to a variety of regional peculiarities such as the favourable meteorological conditions, the extensive supra-glacial debris and the timing of the main precipitation season.

KEY WORDS: Glacier surface mass balance modelling, Debris-covered glaciers, Ice and snow ablation, Karakoram Anomaly.

[1] *Institute of Geography, University of Bern, Hallerstrasse 12, CH-3012, Bern, Switzerland*

[2] *Commission for Geodesy and Glaciology, Bavarian Academy of Sciences and Humanities, Alfons-Goppel Straße 11, D-80539 München, Germany*

[3] *Dipartimento di Scienze della Terra, Università degli Studi di Milano, Via Mangiagalli 34, I-20133, Milano, Italy*

**Corresponding author: A.R. Groos, alexander.groos@giub.unibe.ch*

The field work during summer 2011 and 2013 was organised and funded by the Ev-K2-CNR Association in the framework of the Paprika and SEED projects. We thank the Pakistan Meteorological Department (PMD) for providing meteorological data and the TU Berlin (Department of Ecology, Chair of Climatology) for making the comprehensive High Asia Refined Analysis dataset (HAR) available. SRTM and Landsat data were downloaded from USGS' EarthExplorer and MODIS Snow Cover data from NASA's National Snow and Ice Data Center (NSIDC). The Leibniz Supercomputing Centre in Munich is appreciated for giving access to its Linux-Cluster where the model runs were performed.

Supplementary material as well as all figures and tables presented in this article are stored in the open access library PANGAEA (Groos & alii, 2017). The input raster data as well as the model results are available upon request by email to the first author (alexander.groos@giub.unibe.ch). For the download of the model, please access CRAN - the Comprehensive R Archive Network: https://CRAN.R-project.org/package=glacierSMBM.

INTRODUCTION

The Karakoram in the northwestern part of High Mountain Asia (HMA) is one of the most extensively glacierised areas outside the polar regions (Dyurgerov & Meier, 2005) and has increasingly attracted attention in recent years due to its glaciological and climatological peculiarities. In contrast to the central and eastern Himalaya, where many glaciers have responded to global climate change in the form of ice mass loss and negative length or area changes (e.g. Bolch & *alii*, 2011; Cogley, 2011; Bolch & *alii*, 2012; Kääb & *alii*, 2012; Cogley, 2016), expansion of individual glaciers has repeatedly been reported from the Karakoram based on in-situ and remote sensing observations (Hewitt, 2005; Hewitt, 2011; Rankl & *alii*, 2014). Several satellite-based geodetic measurements provide evidence that the glacial stability, known as Karakoram Anomaly (Hewitt, 2005), is indeed a regional phenomenon dating back to the 1970s (e.g. Gardelle & *alii*, 2012, 2013; Kääb & *alii*, 2015; Rankl & Braun, 2016; Agarwal & *alii*, 2017; Bolch & *alii*, 2017; Zhou & *alii*, 2017). Investigations

on the underlying climatological, glaciological and geomorphological processes causing the anomalous pattern in this remote and complex mountain terrain are hampered by the lack and sometimes limited quality of published observational data (Bolch & *alii* 2012). Frequent glacial surges (Diolaiuti & *alii*, 2003; Hewitt, 2007; Mayer & *alii*, 2011; Rankl & *alii*, 2014; Quincey & *alii*, 2015) and other dynamic processes like avalanches or snow redistribution in the accumulation zone (Hewitt, 2011) further complicate the interpretation of glacier length, elevation and surface mass balance changes (Paul, 2015).

Increasing winter precipitation and decreasing summer temperatures since the beginning of meteorological records (most of them dating back to the 1950s and 1960s) are discussed as possible causes for the Karakoram Anomaly (Archer & Fowler, 2004; Fowler & Archer, 2006; Khatak & *alii*, 2011; Bocciola & Diolaiuti, 2013; Iqbal & *alii*, 2016) as well as the extensive and thick supraglacial debris in the ablation zone of the glaciers (Scherler & *alii*, 2011; Minora & *alii*, 2016). Furthermore, a recent study points out that the Karakoram might generally respond less sensitively to recent climate change due to a characteristic seasonal cycle: the prevailing winter precipitation in the region coincides with air temperatures far below freezing and accumulation is therefore less affected by rising temperatures than the monsoonal summer snowfall in the central and eastern Himalaya, where warming may cause a transition from snow- to rainfall (Kapnick & *alii*, 2014). However, whether favourable climatic conditions or special meteorological and geomorphological mechanisms are the dominant drivers of the Karakoram Anomaly is still uncertain.

As long as the drivers are not better understood, projections of glacier changes in the Karakoram remain uncertain (Bolch & *alii*, 2012). This involves the risk that the impacts of glacial changes in the region on global mean sea level rise (e.g. Gardelle & *alii*, 2012) as well as on the regional hydrological cycle (Immerzeel & *alii*, 2010; Kaser & *alii*, 2010) are unconstrained. Discharge arising from snow and glacial melt in the mountains contributes to more than half of the annual run-off from the region and is a crucial fresh water source for the people living in the semi-arid valleys of the Upper Indus Basin (UIB) (Bookhagen & Burbank, 2010; Immerzeel & *alii*, 2012; Soncini & *alii*, 2015; Pritchard, 2017). The fresh water is primarily used for agricultural irrigation and hydropower generation downstream of the UIB (Mirza & *alii*, 2008; Qureshi & *alii*, 2010; Bocchiola & Soncini, 2017). With an expected strong regional population growth (Feeney & Alam, 2003; United Nations, 2015), water demand for irrigation and the maintenance of hydroelectric power stations will further increase, but even nowadays the supply from the Indus River cannot compensate for the downstream water abstraction (Wada & *alii*, 2011, 2013; Wanders & Wada, 2015).

Even though geodetic measurements based on laser altimetry (e.g. Kääb & *alii*, 2012; Gardner & *alii*, 2013; Kääb & *alii*, 2015) or the differencing of digital elevation models (e.g. Gardelle & *alii* 2012, 2013; Rankl & Braun, 2016) delivered essential information on the extent and timeframe of the Karakoram anomaly, they hitherto do not allow for the estimation of region-wide annual glacier surface mass balances or the distinction between inter-annual changes in accumulation and ablation due to the limited number of satellite overflights.

Field work in remote and fragile mountain areas like the Karakoram is costly, time-consuming and labour-intensive, but nevertheless inevitable to investigate site-specific features like high-altitude accumulation or the influence of debris on glacial melt (e.g. Hubbard & Glasser, 2005). Classical ablation studies in the Karakoram are irregular and restricted to the Biafao (Hewitt & *alii*, 1989; Wake, 1989), Burche (Muhammad & Tian, 2016), Hinarche (Mayer & *alii*, 2010), Baltoro (Mayer & *alii*, 2006; Mihalcea & *alii*, 2006, 2008a) and Siachen glacier (Bhutiyani, 1999). The available measurements are therefore too scarce to extrapolate the results in space and time.

Different numerical models complementing satellite-based and in-situ measurements have been applied in the Karakoram in recent years with the aim to assess the past and future glaciological response to climate change (e.g. Chaturvedi & *alii*, 2014; Kumar & *alii*, 2015). However, the spatial resolution of these models is insufficient to resolve glacier-specific processes. Studies focusing on the modelling of cryosphere-atmosphere interactions or the impact of debris cover on glacial melt are rare and limited to narrow observation periods (Collier & *alii*, 2013, 2015; Minora & *alii*, 2015). The only two available model applications for the region which take ablation as well as accumulation processes into account were designed to investigate climate change impacts on the UIB hydrology (Soncini & *alii*, 2015; Lutz & *alii*, 2016). Detailed spatial evaluations of the glacier surface mass balance and the effects of debris cover on glacial melt are, however, neglected in both studies.

Here, we present a novel and open source high-resolution glacier Surface Mass Balance Model (hereafter glacierSMBM), which takes the insulating as well as amplifying characteristics of supraglacial debris into account. The model is applied on a daily time step from August 2010 until July 2011 with the aim to

i assess the annual accumulation, ablation and surface mass balance in the Karakoram,
ii test whether the model can reproduce the characteristic mass balance pattern in the Karakoram,
iii investigate how sensitively the glaciers respond to modifications of different meteorological and glaciological variables,
iv and to identify and prioritise datasets and processes that should be modified or implemented in future versions of glacierSMBM to increase the accuracy of region-wide mass balance calculations in the Karakoram.

STUDY AREA

The Karakoram (34.1° - 36.9° north, 73.7° - 78.4° east) is located in the northwest of HMA in the borderland of Pakistan, Afghanistan, India and China (see fig. 1). It is surrounded by other high mountain ranges like the Hindu Kush in the west, the Pamir in the further northwest, the Kunlun Shan in the northeast, the Ladack Range in

the southeast and the Himalaya in the south. Although the boundaries of the Karakoram have already been defined by an international conference in 1936/1937 (Mason, 1938), the delineation of the mountain range varies essentially between several glaciological studies (see fig. 1 in Gardelle & *alii*, 2012; Rankl & *alii*, 2014; Minora & *alii*, 2015, 2016). Depending on the selected inventory and the defined boundaries, the number of glaciers in the region varies between 708 and 11,986 and corresponds to a glacierised area of 4,605 and 21,688 km^2, respectively (see tab. 1). Following the boundary suggestions of Mason (1938), the Karakoram comprises an area of 44,334 km^2. On average, the Karakoram rises 4,685 m above sea level (a.s.l.) and includes four 8,000-meter peaks. The glaciers cover an elevation range from <2,500 m a.s.l. to >8,000 m a.s.l., but 80% are located between 4,000 and 5,500 m a.s.l. (Hewitt, 2011). Vast high-altitude accumulation basins cause the formation of some of the largest glaciers outside the polar regions, like the Siachen (~77 km), Biafo (~65 km) and Baltoro glacier (~61 km). In contrast, smaller valley glaciers, cirque glaciers and hanging glaciers are more numerous.

TABLE 1 - Overview of the available glacier inventories for the Karakoram.

Source	Date [Range]	Glacier Number	Glacier Area [km^2]
Bolch & *alii*, 2012	2000-2002	?	17,946
Dyurgerov & Meier, 1997	?	?	16,600
ESA CCI, 2015	1998-2002	11,986	21,688
Minora & *alii*, 2013	2001,2010	708	4,605
Present study	2001,2010	836	7,436
Rankl & Braun, 2014	1976-2012	1,219	?

Surge-type glaciers are another characteristic feature of the Karakoram. The rapid, cyclic and independent advance of individual glaciers has already been noticed several decades ago (Hewitt, 1969). Even though the phenomenon has been studied more systematically in recent years, potential causes and triggers are still under debate (e.g. Diolaiuti & *alii*, 2003; Hewitt, 2007; Copland & *alii*, 2011; Mayer & *alii*, 2011; Rankl & *alii*, 2014; Paul, 2015; Quincey & *alii*, 2015, Round & *alii*, 2016).

Thick debris and supraglacial moraines cover ~10% of the glacier surface area in the Karakoram (Bolch & *alii*, 2012). While snow avalanches from steep slopes play an important role for glacier nourishment, single rockfall events, landslides and mixed avalanches continuously transport debris of different lithologies onto the glaciers (Hewitt, 2005, 2009, 2011; Gibson & *alii*, 2016). Comprehensive in-situ ablation and debris thickness investigations are only available for the Hinarche (Mayer & *alii*, 2010) and Baltoro glacier (Mayer & *alii*, 2006; Mihalcea & *alii*, 2006, 2008a). The debris thickness and grain size varies across the ablation zone and increases towards the glacier terminus. Field measurements indicate that the thickness ranges from few mm (dust) up to several meters (Mayer & *alii*, 2006, 2010), but a debris layer of more than 40-50 cm is difficult to remove and measure.

Precipitation is highly variable across the mountain range and tends to increase exponentially with altitude, even though this is not valid for all sub-basins (e.g. Winiger & *alii*, 2005; Dahri & *alii*, 2016). More than 90% of the annual precipitation above 5,000 m a.s.l. is deposited as snow (Winiger & *alii*, 2005; Maussion & *alii*, 2014). At the Biafo glacier in the central Karakoram maximum snowfall occurs between 4,900 m and 5,400 m a.s.l. (Hewitt & *alii*, 1989; Wake, 1989), but these findings may not be representative for other accumulation areas in the region. At four selective sites (Bagrot valley, Baltoro glacier, Biafo glacier, Urdok glacier), information on snow accumulation from either snow pits, ice cores or radar measurements are available. Annual accumulation ranges from approximately 1,000 mm to 2,000 mm water equivalent (w.e.) (Hewitt & *alii*, 1989; Wake, 1989; Winiger & *alii*, 2005; Hewitt, 2011; Mayer & *alii*, 2014). Even though snowfall induced by intrusions of the South Asian Monsoon sometimes occurs during the ablation period, the seasonal cycle in the Karakoram is dominated by the west wind circulation and prevailing winter precipitation (Winiger & *alii*, 2005; Bookhagen & Burbank, 2010; Maussion & *alii*, 2014; Mayer & *alii*, 2014).

The Baltoro glacier, located in the central Karakoram, is the only glacier in the region where glaciological, geomorphological and meteorological in-situ data are concurrently available. For this reason, data from this glacier serve as basis for the calibration and validation of the model.

DATA AND DERIVED PARAMETERS

For the application of the distributed glacier surface mass balance model, spatial information on the meteorological conditions and glacier surface characteristics are necessary. A combination of in-situ measurements, remote sensing products and reanalysis data is used to generate the input variables and parameters for the model. The processing of the base data and the generation of input datasets is described in the following sections.

Automatic Weather Stations

The number of permanent AWS in the Karakoram has steadily increased during the last thirty years (a comprehensive overview is provided by Dahri & *alii*, 2016). However, most of them are located in the semi-arid valley basins and are not representative for the entire mountain range (Miehe & *alii*, 2001; Winiger & *alii*, 2005). A few additional high elevation AWS were installed within the research projects EV-K2-CNR (Bocchiola & *alii*, 2011; Bocchiola & Diolaiuti, 2013) and Culture Area Karakoram (Winiger & *alii*, 2005). Only meteorological data from eight AWSs of the Pakistan Meteorological Department (PMD) and two of the EV-K2-CNR project – covering an elevation range from 1,255 m (Chilas) to 4,060 m a.s.l. (Urdukas) – are considered in this study (see tab. 2) due to obstacles in data acquisition.

TABLE 2 - Location of AWS in the Karakoram or adjacent regions considered in this study.

Station	Location	Lon [°]	Lat [°]	Altitude [m]	Record	Resolution	Source
1	Askole	75.816	35.682	3,040	2004-2011	hourly	EV-K2-CNR
2	Astor	74.867	35.363	2,168	1980-2009	monthly	PMD
3	Babusar	74.053	35.209	2,854	2006-2009	monthly	PMD
4	Bunji	74.635	35.642	1,470	1980-2009	monthly	PMD
5	Chillas	74.099	35.415	1,255	1980-2009	monthly	PMD
6	Gilgit	74.284	35.920	1,461	1980-2009	monthly	PMD
7	Gupis	73.445	36,231	2,156	1980-2009	monthly	PMD
8	Hunza	74.660	36.324	2,374	2007-2009	monthly	PMD
9	Skardu	75.526	35.330	2,230	1993-2009	monthly	PMD
10	Urdukas	76.286	35.728	4,060	2004-2011	hourly	EV-K2-CNR

Field Data

Intensive field work was carried out on the Baltoro glacier during the ablation seasons 2011 and 2013 to obtain meteorological data and to measure ablation, debris thickness and snow accumulation.

ACCUMULATION STUDIES - Individual annual precipitation measurements in the Karakoram are restricted to elevations below 5,000 m a.s.l. since no permanent AWSs are installed further up. Snow pits in the accumulation zone of the Baltoro glacier (see fig. 1) were therefore explored at an altitude of ~6,100 m a.s.l. in summer 2013 to calculate annual snowfall rates from the density of consecutive stratigraphic firn layers. The mean annual accumulation at this location for the period 2001-2013 is ~1,400 mm w.e. and the standard deviation (sd) is ~250 mm.

ABLATION AND DEBRIS THICKNESS - Glacial melt rates were obtained on the Baltoro glacier during summer 2011 (22nd July - 10th August). 16 ablation stakes were drilled into the glacier ice and distributed over a distance of ~30 km and an elevation of ~900 m (3,700 m to 4,600 m a.s.l.) to account for the varying debris thickness and melt rates across the ablation zone (see tab. 3). At the respective ablation stake, the debris thickness was determined by excavating the coarse gravel until the glacier surface, measuring the height above the glacier surface and depositing it again.

Melting Factors

To assess the melt rate of ice and snow, melting factors are calculated from measured ablation and interpolated air temperature or net radiation of the High Asia Refined Analysis (HAR) dataset (see section *Reanalysis Data*) over the same period (Hock, 2003):

$$TMF = \frac{\sum_{i=1}^{n} M}{\sum_{i=1}^{n} T^{+} \Delta t} \quad (1)$$

where TMF is the temperature melting factor (m d^{-1} $°C^{-1}$), M is the ice or snow melt (m) and T^{+} is the cumulative temperature above freezing (°C) during a period of n time intervals, Δt *(d)*. For the calculation of the radiative melting factor RMF (m d^{-1} W^{-1} m^2), T^{+} is replaced by the cumulative positive net radiation NR^{+} (W m^{-2}). Ablation of bare ice was only measured at one selective site of the Baltoro glacier (stake 2, tab. 3). An ice melt of 61.5 cm and a positive degree-day sum of 92 °C between 23rd July and 7th August 2011 yield a temperature melting factor (TMF_{Ice}) of 6.7 mm d^{-1} $°C^{-1}$. This finding is in agreement with an independently calibrated TMF_{Ice} of 7.1 mm d^{-1} $°C^{-1}$ for debris-free glaciers in the same region (Lutz & *alii*, 2016). TMFs for snow are generally lower than those for ice (Hock, 2003; Zhang & *alii*, 2006; Huintjes & *alii*, 2010; Soncini & *alii*, 2015, 2016), but have not been determined in the Karakoram. According to ratios and values found in the literature, a TMF_{Snow} of 4.5 mm d^{-1} $°C^{-1}$ (2/3 of TMF_{Ice}) seems reasonable (Hock, 2003; Zhang & *alii*, 2006; Lutz & *alii*, 2016). A radiative melting factor (RMF_{Ice}) for debris-free areas of 0.079 mm d^{-1} W^{-1} m^2 is adopted from Minora & *alii* (2015). Using the same 2/3-ratio as before, the RMF_{Snow} is set to 0.053 mm d^{-1} W^{-1} m^2.

Remote Sensing Data

A set of different remote sensing products (SRTM DEM, Landsat 5, MODIS Snow Cover) is explored to obtain spatial information on the glacier elevation, debris thickness distribution, temporal snow cover variability and shift of transitional snow line altitudes.

GLACIER INVENTORY - This study draws on a glacier inventory for the Central Karakoram National Park developed by Minora & *alii* (2013) because it provides glacier outlines for the selected modelling period. 128 additional glaciers (2,831 km^2) are included by manual editing of two Landsat 5 images (ID 3 and 4 in tab. 4) in combination with the DEM and high-resolution images from Google Earth. The new inventory (see fig. 1) comprises altogether 836 glaciers, but does not contain those in the border areas in the west, north and southeast of the mountain range.

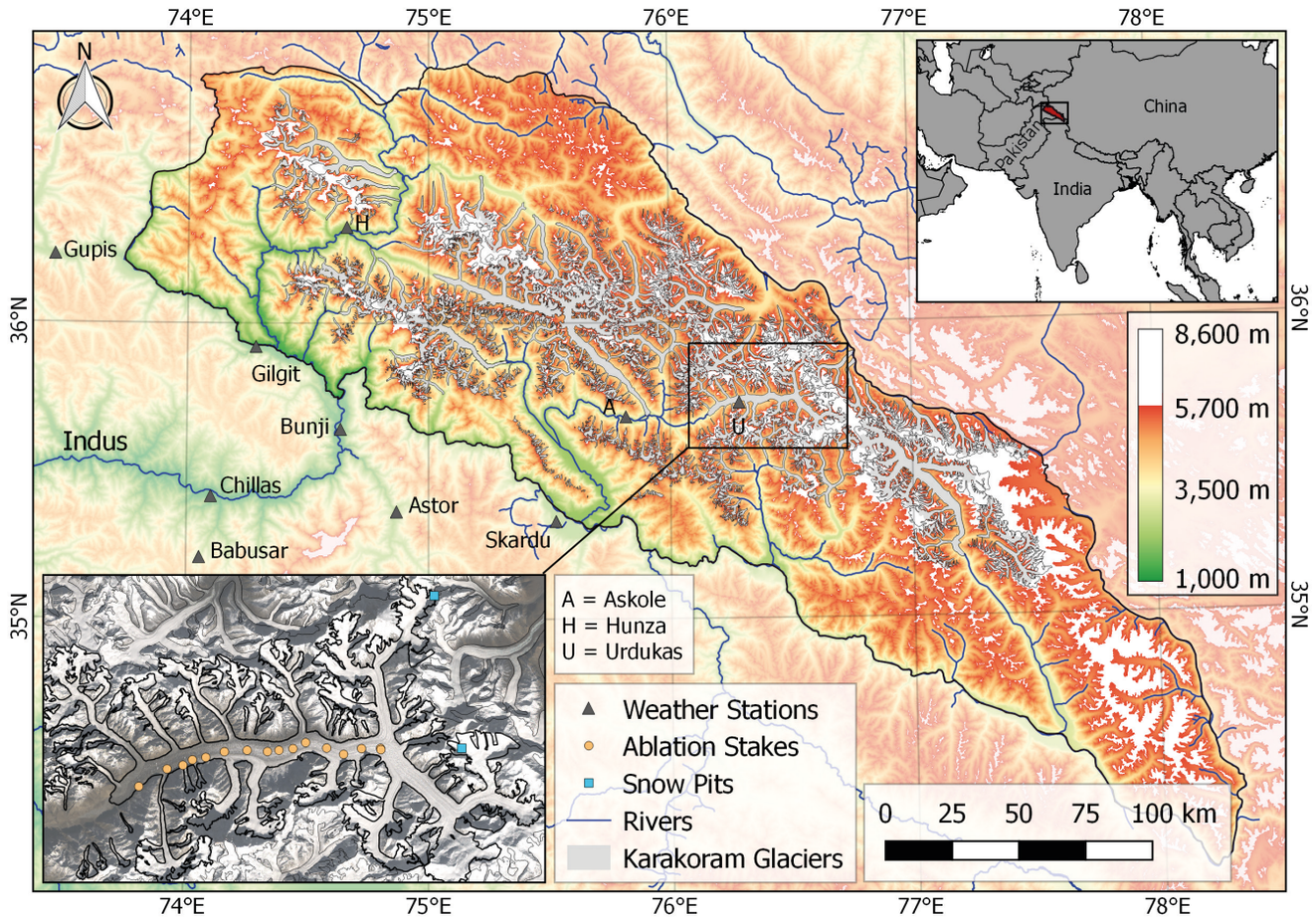

FIG. 1 - Location and topography of the Karakoram in the northwestern part of High Mountain Asia. The delineation of the mountain range follows the recommendations of the Karakoram Conference hold in 1936-1937 (Mason, 1938). All glaciers included in the inventory from 2010 are highlighted in grey. Ablation and accumulation measurements on the Baltoro glacier during field work in 2011 and 2013 are displayed in the lower left corner.

TABLE 3 - Overview of the sub-debris ablation measurements on the Baltoro glacier between 22nd July and 10th August 2011. D_T = debris thickness.

Stake	Lon [°]	Lat [°]	Altitude [m]	Start	End	D_T [cm]	$Melt_{total}$ [cm]	$Melt_{rate}$ [cm. d^{-1}]
1	76.516	35.741	4,571	22.07.	07.08.	9.5	34.0	2.1
2	75.516	35.739	4,556	23.07.	07.08.	0.0	61.5	4.1
3	76.490	35.741	4,502	24.07.	08.08.	3.5	57.0	3.8
4	76.466	35.735	4,440	24.07.	08.08.	2.2	66.2	4.4
5	76.444	35.742	4,375	24.07.	08.08.	2.0	63.0	4.3
6	76.416	35.748	4,330	24.07.	08.08.	3.3	57.8	3.9
7	76.399	35.742	4,293	25.07.	08.08.	8.8	53.4	3.8
8	76.380	35.740	4,239	25.07.	08.08.	5.0	40.1	2.8
9	76.365	35.739	4,202	25.07.	08.08.	3.5	65.0	4.6
10	76.338	35.740	4,164	26.07.	09.08.	5.6	53.8	3.9
11	76.307	35.739	4,075	26.07.	09.08.	12.6	33.9	2.5
12	76.283	35.733	3,996	27.07.	09.08.	26.0	25.0	1.9
13	76.265	35.731	3,957	28.07.	09.08.	13.0	30.0	2.5
14	76.231	35.721	3,838	29.07.	10.08.	31.5	14.0	1.2
15	76.252	35.725	3,917	29.07.	10.08.	12.0	32.0	2.9
16	76.193	35.703	3,704	30.07.	10.08.	37.5	11.5	1.1

TABLE 4 - Selection of Landsat 5 images used for the calculation of debris thickness and the determination of glacier surface characteristics.

ID	Scene	Path	Row	Acquisition Date	Cloud Cover [%]
1	LT51480352010235KHC00	148	35	2010-08-23	4
2	LT51490352010290KHC00	149	35	2010-10-17	5
3	LT51480352011222KHC00	148	35	2011-08-10	8
4	LT51490352011229KHC00	149	35	2011-08-17	58

DIGITAL ELEVATION MODEL - A high-resolution digital elevation model (DEM) for the study area is generated from nine tiles of SRTM 1 Arc-Second Global data with a horizontal resolution of ~30 m (Rabus & *alii*, 2003). The few existing voids are filled using inverse distance weighting.

GLACIER SURFACE CHARACTERISTICS - Four Landsat 5 scenes (see tab. 4) with a spatial resolution of 30 m are processed to obtain information on the glacier surface characteristics and debris thickness distribution. All spectral bands are converted from digital numbers into spectral radiances (W m^{-2} sr^{-1} μm^{-1}) and finally into surface reflectance (Barsi & *alii*, 2007; NASA, 2011). Atmospheric parameters required for the correction of atmospheric obstructions are calculated with the NASA Atmospheric Correction Parameter Tool (Barsi & *alii*, 2003, 2005).

Two Landat 5 scenes (ID 1 and 2 in tab. 4) from the 23rd of August and 17th of October 2010 serve for the determination of the glacier surface characteristics at the beginning of the modelling period. Perennial snow in the accumulation areas is discriminated from bare ice and debris by applying a single threshold to the mean surface reflectance of the three Landsat 5 bands in the visible light. Snow is defined by a mean reflectance greater than 0.53 based on a manual evaluation of the images. A combination of the reflectance in the short-wave infrared (1,550-1,730 nm, band 5) and in the visible spectrum (e.g. 530-600 nm, band 2) is used to distinguish between debris cover and bare ice using the Normalised Difference Snow Index (NDSI):

$$NDSI = \frac{(B2 - B5)}{(B2 + B5)} \quad (2)$$

where B2 is the green and B5 is the shortwave infrared band of Landsat 5. For the snow-free areas, a NDSI above 0.2 is defined as debris and below as ice based on the visual inspection of the visible bands.

DEBRIS THICKNESS - The extent and variability of supraglacial rock cover makes it difficult to obtain distributed information on the debris thickness for glacier areas. While individual in-situ debris thickness measurements are not representative for the entire glacier area, they can serve for the calibration of satellite imagery. This has been proven by recent studies, which found a good correlation between measured debris thickness and remotely sensed surface temperature (Mihalcea & *alii*, 2008b). The empirical relationship between both variables has been used for the spatial extrapolation of debris thickness over the entire glacier area (Mihalcea & *alii*, 2008a, 2008b; Minora & *alii*, 2015). Spectral radiances of the ASTER or Landsat thermal infrared bands are converted into surface temperatures using an inverted Planck function (e.g. Coll & *alii*, 2010):

$$T_S = \frac{K_2}{ln\left(\frac{K_1}{L_\lambda} + 1\right)} \quad (3)$$

where T_s is the surface temperature, K_1 and K_2 are constant values (607.76 W m^{-2} sr^{-1} μm^{-1} and 1,260.56 K, respectively; NASA, 2011) and L_λ are spectral radiances. In accordance with findings from Minora & *alii* (2015), an exponential function describes best the relationship between debris thickness (D_T) and glacier surface temperature (T_s). D_T-measurements from 16 ablation stakes distributed across the Baltoro glacier during 2011 (see. tab. 3) and a Landsat thermal infrared image (ID 3 in tab. 4) from the same period, covering the Baltoro region and eastern Karakoram, serve for the region-wide debris thickness calculation. Based on the evaluation of non-linear least squares, the best-fitting equation with a standard error (S) of 7.9 cm (S = 3.9 cm, if two outliers are excluded) is:

$$D_T = exp(0.16T_S - 44.67) \quad (4)$$

The obtained empirical relationship is not transferable to other regions like the western part of the Karakoram due to the lack of necessary field measurements and the varying meteorological conditions during and before the respective acquisition. Other studies extended the empirical approach and introduced a surface energy-balance model with distributed meteorological and surface temperature input data to calculate the debris thickness as a residual of energy fluxes (Foster & *alii*, 2012; Rounce & McKinney, 2014; Schauwecker & *alii*, 2015). Here we follow the concept of Rounce and McKinney (2014) to obtain debris thickness information for all glaciers of the inventory. Surface temperatures in Kelvin derived from two thermal Landsat 5 images (ID 3 and 4 in tab. 4) in combination with hourly meteorological data from the HAR dataset (see section *Reanalysis Data*) are used as input for the steady-state surface energy balance model:

$$R_n + LH + H - Q_c = 0 \quad (5)$$

where R_n is the net radiation flux (see section *Global Radiation*), LH is the latent heat flux (assumed to be zero), H is the sensible heat flux (see original paper) and Q_c is the ground heat flux (all in W m^{-2}):

$$Q_c = G_{ratio} \frac{k_{eff}(T_s - 273.15)}{D_T} \quad (6)$$

G_{ratio} is a factor used to approximate the nonlinear temperature variation in the debris layer. A value of 2.7 for G_{ratio} and 0.96 W m^{-1} K^{-1} for the effective thermal conductivity (k_{eff}) is adopted from Rounce & McKinney (2014) because information on specific debris properties like the lithological composition or the fraction of air and water is highly variable and has not been investigated in the Karakoram up to now. The final equation for the debris thickness calculation is:

$$D_T = \frac{G_{ratio} k_{eff}(T_s - 273.15)}{R_n + H} \quad (7)$$

Both approaches (Eqn 4 & 7) can hardly distinguish between debris thickness values of >0.4 m since the influence of glacier ice on T_s decreases exponentially with debris thickness (Mihalcea & *alii*, 2006; 2008a). Melt rates below a thick debris layer are, vice versa, generally low so that the limitation of the approach is negligible.

Transitional Snow Line Altitude - A region-wide spatial evaluation of glacier surface mass balance model outputs is often challenged by data scarcity in high mountain areas. Seasonal elevation shifts of supraglacial snow cover are controlled by the interaction of snow accumulation and ablation and therefore reflect the temporal evolution of both glacier mass balance components. Remotely sensed transitional line altitudes (TSLAs) are explored in this study to test the plausibility and variability of the modelled mass balance results (see section *Model Validation*). The MODIS Snow Cover Product (MOD10_L2) with a spatial resolution of 500 m (Hall & *alii*, 2002; Hall & Riggs, 2007) is used to create binary snow cover maps (1 = snow, 0 = no snow) for the Karakoram on a daily basis. Cloudy pixels are neglected for further analysis and scenes with cloud obstructions of more than 20% are not considered at all. Subsequently, the relation of snow vs. snow-free areas is calculated iteratively for elevation bands of 50 m, which were extracted from the SRTM DEM (resampled to a 500 m horizontal resolution using the mean of all 30-m pixels within each 500-m pixel). The manual delineation of supraglacial snow on Landsat images confirms that the lowest elevation band of each snow cover map with a snow-cover fraction of >50% is suitable to define the snow line altitude.

Reanalysis Data

Daily interpolated meteorological data of the High Asia Refined Analysis (HAR) are used and are applied for glaciological studies in the Karakoram for the first time. HAR is a new gridded meteorological dataset developed by Maussion & *alii* (2014). The Advanced Weather and Research Forecasting model (WRF-ARW) was run with the output of the Global Forecast System of the National Center for Environmental Information (NCEP GFS) to generate the HAR dataset (Maussion & *alii*, 2014). It is available in hourly and daily resolution from October 2000 until September 2014 and covers the entire Himalaya, Pamir and Karakoram. The spatial resolution is 10 km for the High Asia domain (HAR10). All necessary HAR10-variables (see tab. 5) are reprojected into UTM43N and interpolated to the Landsat grid with a spatial resolution of 30 m.

Table 5 - Variables of the High Asia Refined Analysis dataset (HAR) used as meteorological input for glacierSMBM or the calculation of the debris thickness distribution.

Variable	Description	Unit	Time Step	Type
hgt	terrain height	m	-	static
netrad	surface net radiation	W m^{-2}	daily, hourly	2d
prcp	total precipitation	mm h^{-1}	daily	2d
psfc	surface air pressure	Pa	hourly	2d
t2	air temperature at 2 m	K	daily, hourly	2d

Precipitation - The original HAR dataset overestimates precipitation in the dry valley basins of the Karakoram as a comparison with rain gauge records from the Askole and Urdukas AWS shows (see fig. 2). A vertical correction is applied to account for the postulated exponential increase of precipitation with altitude (Winiger & *alii*, 2005). The offset between the annual HAR-precipitation and the measured one at the Askole AWS (3,040 m a.s.l.), Urdukas AWS (4,060 m a.s.l.) and the snow pit (6,100 m a.s.l.), respectively, serve for the development of elevation-dependent tuning factors. Following this approach, the precipitation tuning factor for elevations ≤3,040 m a.s.l. (Askole AWS) is 0.37, at 4,060 m a.s.l. 0.40 and for elevations ≥6,100 m a.s.l. 0.97 (snow pit). The relationship between the derived tuning factors and altitude is approximated with an exponential function. A general correction map for the modification of the daily precipitation input is finally generated from the elevation-dependent tuning factors and the height information of the DEM.

Air Temperature - The 10 km resolution of the HAR dataset does not resolve the complex topography of the Karakoram and its impacts on air temperature and pressure distribution. Temperatures in the accumulation areas are therefore generally too high and those in the valleys too low. We calculate the elevation difference (DEM_{Diff}) between the resampled HAR DEM and the high-resolution SRTM DEM and use this information together with empirical atmospheric lapse rates (Γ) to apply a vertical correction to the daily HAR temperature input (T_{HAR}):

$$T_{2m} = T_{HAR} + (\Gamma DEM_{Diff}) \quad (8)$$

Monthly mean temperature lapse rates are obtained from the slope of a linear regression of temperature vs. elevation based on data of eight PMD AWS between 1,255 and 2,854 m a.s.l. in the Karakoram. Monthly lapse rates are given priority over an annual or constant lapse rate since the evaluation of temperature records from the

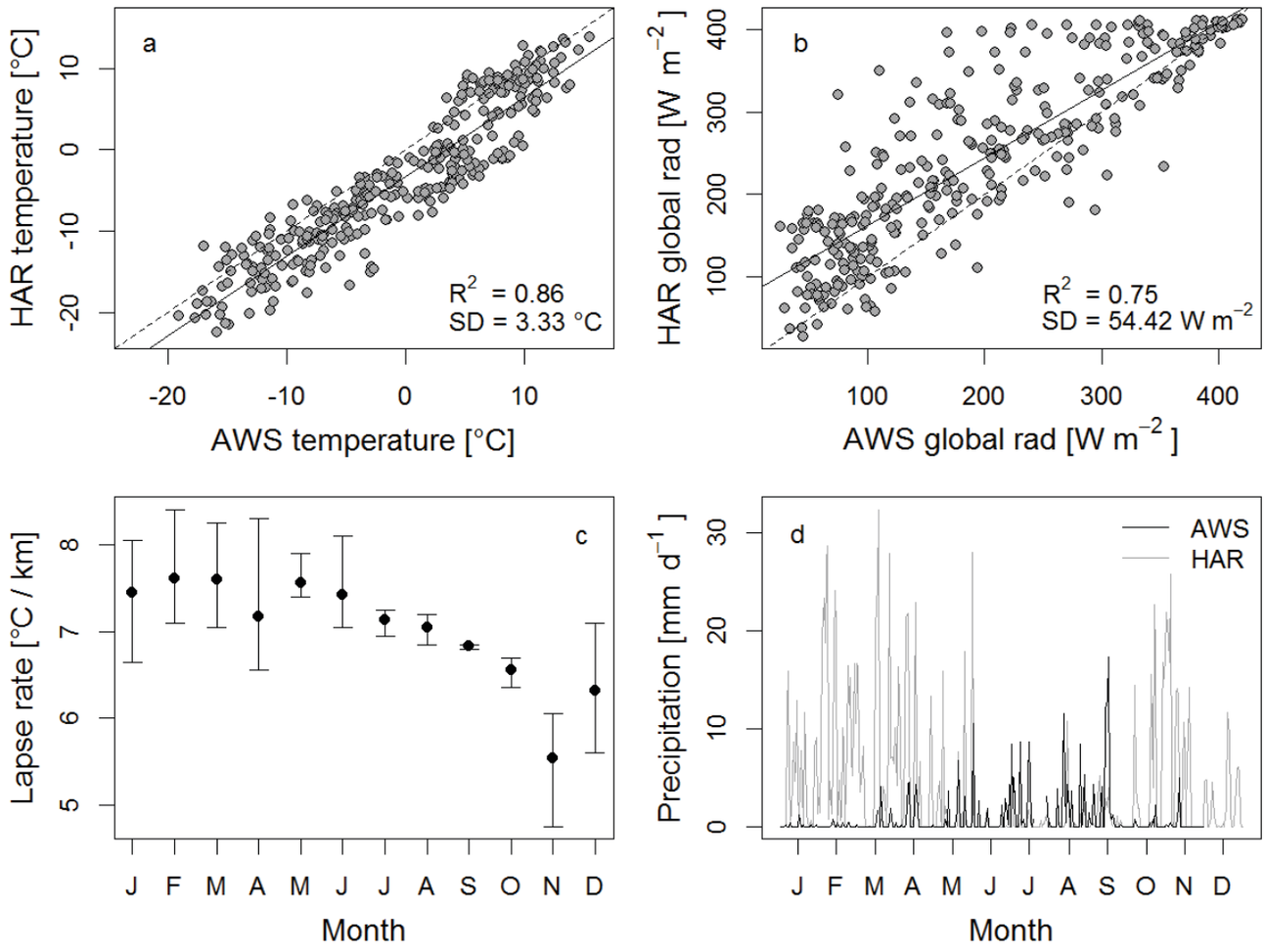

FIG. 2 - Daily mean air temperatures measured at the Urdukas AWS (4,060 m a.s.l.) next to the Baltoro glacier during 2011 vs. interpolated daily mean air temperatures from the HAR dataset (a). Daily global radiation detected at the Urdukas AWS vs. resampled incoming shortwave radiation of the HAR dataset during 2011 (b). Mean monthly temperature lapse rates in the Karakoram (c) calculated from vertical gradients of eight PMD AWS for the period 2007-2009 (the three-year range is indicated by the bars). Measured daily precipitation at the Urdukas AWS vs. corrected and interpolated precipitation from the HAR dataset (d).

considered AWS in the Karakoram indicates that the intra-annual variability of vertical temperature gradients is higher than their inter-annual difference (see fig. 2).

GLOBAL RADIATION - In the current version of the model, HAR net radiation is resampled to 30 m, but neither corrected for shading effects of clouds and topography nor for varying albedo characteristics of different glacier surfaces.

GLACIER SURFACE MASS BALANCE MODEL & APPLICATIONS

glacierSMBM

The glacier Surface Mass Balance Model (glacierSMBM) applied in this study consists of statistical as well as physical components to describe the processes of glacier mass gain and mass loss (see fig. 3). With the development of the model in the open source language R (R Core Team, 2017), the presented approach is reproducible and can be modified for other study areas or purposes. To import, process and export spatial data, glacierSMBM is built upon the R-packages *sp* (Pebesma & *alii*, 2016), *raster* (Hijmans & *alii*, 2016) and *rgdal* (Bivand & *alii*, 2017).

We use distributed air temperature, net radiation and precipitation data with a resolution of 30 m as daily meteorological input for glacierSMBM (see section *Reanalysis Data*). Information on glacier outlines, distributed debris thickness and the initial extent of snow, debris-free and debris-covered ice are required in addition (see section *Remote Sensing Data*). Using this data input, the model calculates accumulation and ablation for each day and pixel. The initial snow mask is updated with every iteration depending on the spatial variation of the modelled snow cover.

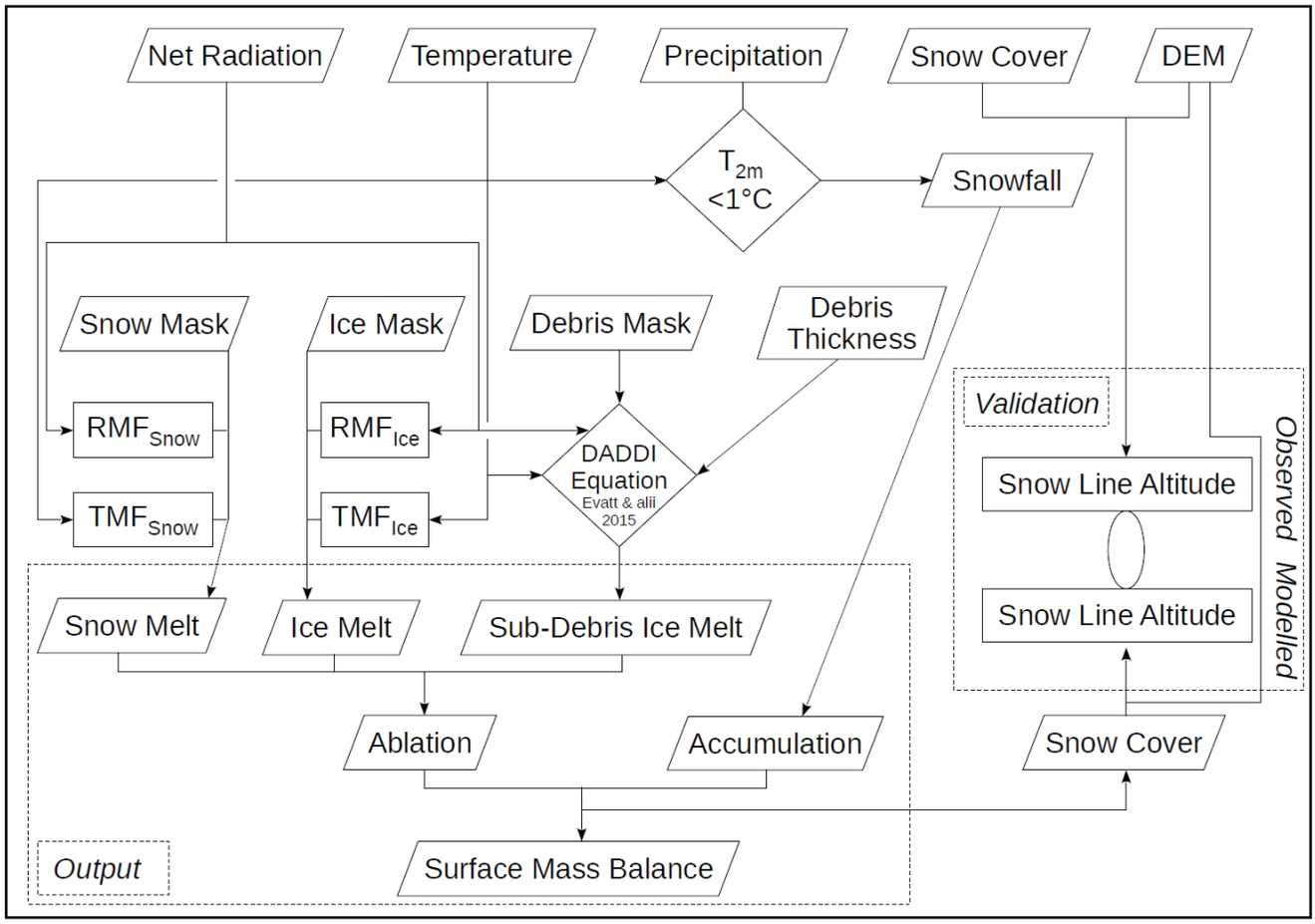

FIG. 3 - Setup of glacierSMBM. RMF and TMF are the radiative and temperature melting factors, respectively.

ACCUMULATION - Daily snowfall (*SF*) in glacierSMBM is defined as precipitation (*Precip*) at air temperatures (T_{2m}) ≤1 °C (Rohrer & Braun, 1994):

$$SF = \begin{cases} 0 & , T_{2m} > 1°C \\ Precip & , T_{2m} \leq 1°C \end{cases} \quad (9)$$

The glacier mass contribution of rainfall (precipitation at $T_{2m} > 1$ °C) is assumed to play no major role in the Karakoram due to the dominance of winter precipitation (Winiger & *alii*, 2005; Maussion & *alii*, 2014). Snowfall over the glacier area is therefore the only source for accumulation (A_{Snow} = *SF*) in the model since mass input from avalanches and wind redistribution has not been implemented yet.

ABLATION - An enhanced degree-day model (e.g. Hock, 2003, 2005; Pellicciotti & *alii*, 2005) is applied to quantify the glacier mass loss ascribed to melted snow (M_{Snow}) and debris-free ice (M_{Ice}):

$$M_{Snow} = \begin{cases} TMF_{Snow}T^{+} + RMF_{Snow}NR^{+} & , T_{2m} > 0°C \\ 0 & , T_{2m} \leq 0°C \end{cases} \quad (10)$$

where TMF_{Snow} and RMF_{Snow} are the empirically determined temperature and radiative melting factors for snow (see section *Melting Factors*), respectively, which are taken as constant in space and time (Hock, 1999). T^{+} is the positive daily mean air temperature (°C) at 2 m height and NR^{+} is the positive net radiation (W m^{-2}). For the calculation of debris-free ice melt (M_{Ice}), those for ice (TMF_{Ice} and RMF_{Ice}) replace the melting factors for snow. Ablation does only occur in the model at air temperatures above freezing because the complex process of percolation, retention and refreezing of meltwater draws from the computational power and has not been parametrised yet.

An initial surface mask (see section *Glacier Surface Characteristics*) distinguishes between firn, debris-free and debris-covered glacier areas. The extent and height of the supraglacial snow changes with time due to the interplay of snow accumulation (Eqn 9) and snow melt (Egn 10). Ablation of debris-free (Eqn 10 with melting factors for ice) or debris-covered glacier ice (Eqn 11-16) sets in as soon as the overlying snow pack is completely melted and takes place as long as a pixel is snow-free. For the quantification of sub-debris ice melt, simple melting factors as for snow and bare ice are not suitable due to the non-linear relation-

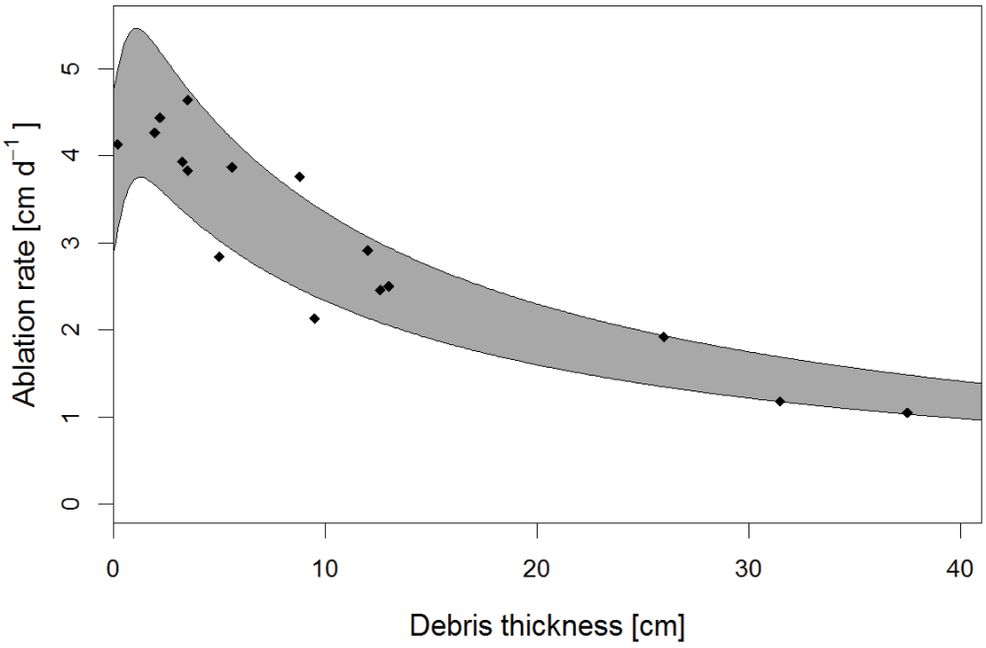

FIG. 4 - Modelled and measured sub-debris ice melt on the Baltoro glacier from 22nd July until 10th August 2011. Empirical melt rates (black diamonds) are obtained from ablation stake readings at selective sites on the glacier with varying debris thickness. Interpolated daily mean air temperature and net radiation from the HAR dataset at the position of the ablation stakes are used as input for Eqn 11 with the configuration described in tab. 6. The grey area displays the range of modelled ablation rates as a function of debris thickness depending on the varying energy input at the different stake locations.

ship of debris thickness and the ice melt below (see fig. 4). Hence, we implement and test the DADDI-Equation (Eqn 11), a novel theoretical model of glacial melt under a porous debris layer ($M_{Sub\text{-}Debris}$) developed by Evatt & *alii* (2015), that has been proven to reproduce the characteristic features of the empirical Østrem curve (Østrem, 1959):

$$M_{\text{Sub-Debris}} = \frac{\nu_1}{1+\nu_2 D_T} - \frac{\mu_1}{\mu_2 + e^{\gamma D_T}} \tag{11}$$

where D_T is the debris thickness (see section *Debris Thickness*) and the other constants are defined as

$$\mu_1 = \frac{L_v u_*^2 (q_h - q_m) e^{-\gamma x_r}}{(1-\phi)\rho_i L_m u_r} \tag{12}$$

$$\mu_2 = \frac{(u_m - 2u_r) e^{-\gamma x_r}}{u_r} \tag{13}$$

$$\nu_1 = \frac{NR^+ + \beta T^+}{(1-\phi)\rho_i L_m} \tag{14}$$

$$\nu_2 = \frac{\beta + 4\varepsilon\sigma T_{freezing}^3}{k} \tag{15}$$

$$\beta = \frac{\rho_a c_a u_*^2}{u_m - u_r(2 - e^{\gamma x_r})} \tag{16}$$

An overview of the units and values of the respective parameters and variables is given in tab. 6 (for more details on the derivation of the DADDI-Equation see the original publication of Evatt & *alii*, 2015).

SURFACE MASS BALANCE - The surface mass balance (*MB*) is calculated for each pixel of the glacier inventory by aggregating the daily difference between snow accumulation and glacial ablation:

$$MB = \sum_{d=1}^{n} A_{Snow} - M_{Snow} - M_{Ice} - M_{\text{Sub-Debris}} \tag{17}$$

Surface mass balances for the entire Karakoram and individual glaciers are finally obtained from area averages based on the outlines defined in the inventory.

Model Calibration

An overall calibration of the model is not feasible due to the lack of glaciological and geodetic mass balance studies in the Karakoram. Therefore, we use simple distributed tuning factors to fit precipitation to the few existing in-situ observations in the accumulation zone of the Baltoro glacier. Melting factors for the enhanced degree-day model are not modified since they were investigated directly in the field. The thermal conductivity (in Eqn 15) of supraglacial debris depends on the lithological composition of the layer (e.g. Conway & Rasmussen, 2000; Reid & Brock, 2010) and is tuned to fit modelled sub-debris ice melt rates to the ones measured on the Baltoro glacier during the ablation season 2011 (see fig. 4).

Model Validation

The number of in-situ accumulation and ablation measurements in the Karakoram is not sufficient to assess the overall accuracy of the modelled glacier surface mass balances. Furthermore, the few observations from the Baltoro glacier were already used for the calibration of the melting factors and debris thickness. We therefore explore two new approaches to test the plausibility, magnitude and variability of the model output:

1. The annual surface mass balance is calculated separately for the upper part of the Baltoro glacier and compared to the estimated average ice volume flow at Concordia (see fig. 6). The maximum ice thickness at Concordia in 4,500 m a.s.l. is ~860 m (Mayer & *alii*, 2006) and the mean velocity obtained from feature-tracking of Landsat 5 images along a profile of ~2,300 m is ~90 m a^{-1}. Assuming a simple parabola for the glacier shape and taking the ice thickness, profile length and velocity into account, the long-term mean ice volume flow at Concordia under equilibrium conditions would be ~0.1164 km^3. This value serves as rough reference for the glacierSMBM output above the profile.
2. Transitional snow line altitudes in the Karakoram derived from MODIS imagery (see section *Transitional Snow Line Altitude*) are compared with those from the model output to evaluate the spatio-temporal shift of the snow line, which represents the interplay of mass build-up and loss on the glaciers.

HAR evaluation

The two HAR-variables air temperature and precipitation (see tab. 5) as main drivers of the glacier mass balance are evaluated at two pixels/locations (~4,060 m a.s.l.) in the western and central Karakoram (Batura and Baltoro glacier, respectively) for the available period 2001-2014 to examine whether the modelling year represents average climatic conditions or coincides with a meteorological extreme. Degree-day sums (accumulated positive air temperatures) in °C and bare ice melt in mm w.e. are calculated for the main ablation period (June-September) of each year. Annual accumulation is approximated from precipitation during the main precipitation season (January-April).

Sensitivity Analysis

To analyse how sensitively the Karakoram glaciers respond to input data uncertainties and future meteorological or glaciological changes, different model configurations and datasets are tested for the Baltoro glacier. Precipitation, temperature and net radiation as main meteorological mass balance drivers are modified since increasing precipitation and rising temperatures in the UIB are projected for the next decades (Lutz & *alii*, 2014). Kapnick & *alii* (2014) argue that accumulation in the Karakoram responds less sensitively to recent climate change because snowfall during winter at temperatures far below zero degrees as observed in the region is less affected by rising temperatures than the monsoonal snowfall in the central and eastern Himalaya. We shift precipitation in the sensitivity analysis by six months in order to simulate a monsoonal precipitation regime and to test whether the hypothesised timing of precipitation has an impact on the glacier mass balance. Summer precipitation is to a lesser extent also observed in the Karakoram (Mayer & *alii*, 2014), but it is not clear yet how climatic changes will affect accumulation during the different seasons in the region. Melting factors as well as the thermal conductivity of debris are taken as constant in space and time, but may vary between different locations (e.g. Hock, 2003; Gibson & *alii*, 2016) and are therefore evaluated regarding their impact on ablation. The effects of debris thickness on glacial melt are investigated by simulating the surface mass balance of the Baltoro glacier for two conditions: a thickness doubling and a debris-free glacier tongue.

RESULTS

Meteorology

The mean air temperature (2001-2014) during the main ablation season (June-September) at the Batura and Baltoro glacier in ~4,060 m a.s.l. derived from the HAR dataset is 5.0 and 4.8 °C, respectively. This corresponds to a mean degree-day sum of 676 and 654 °C and bare ice melt of ~4,500 and ~4,400 mm (w.e.). During the modelling period (2010 – 2011), the mean June-September air temperature exceeds the multi-annual June-September average by 0.8 and 0.6 °C (corresponding to an additional ice melt of ~700 and ~500 mm w.e.), respectively, what is less than the inter-annual variability (sd = 1.2 and 1.6 °C). The mean annual precipitation (2001-2014) differs between the western Batura (1,059 mm; sd = 224 mm) and central Baltoro glacier (721 mm; sd = 147 mm), but at both locations, the mean accumulation difference (+47 and +26 mm) between the modelling period and long-term average is negligible. Accordingly, the selected glacier mass balance year represents average meteorological conditions in the region with a slightly warmer ablation season.

Calculated monthly mean lapse rates for the Karakoram range from 5.53 °C km^{-1} in November to 7.6 °C km^{-1} in February (see fig. 2). During the main ablation season (June-September) the intra-annual variability of the lapse rates is low (standard deviation = 0.12 °C). The calculated mean annual lapse rate for the Karakoram is 7.2 °C km^{-1} and matches with the vertical temperature decrease of 6.3 – 7.5 °C km^{-1} measured on the Baltoro glacier (Mihalcea & *alii*, 2006; Mayer & *alii*, 2010). Distributed daily air temperatures interpolated from the HAR dataset show a good correlation with the observations at the two high-elevation AWS Urdukas and Askole (R^2 = 0.86 and 0.83, respectively), especially during the ablation season. However, they underestimate the annual mean temperature by 3.27 and 3.42 °C, respectively, due to a negative bias in spring and autumn. The region-wide mean annual air temperature for the Karakoram (in 2011) based on the HAR dataset is -8.3 °C, with the warmest days occuring in August (region-wide mean maximum = 9.8 °C) and the coldest

ones in January (region-wide mean minimum = -25.7 °C). In addition to the distinct seasonal cycle, strong lateral temperature gradients between peaks and valleys of >40 °C 10 km^{-1} are common during the whole year. The annual 0 °C isotherm is located at ~3,500 m (a.s.l.).

The daily incoming shortwave energy flux of the HAR net radiation is compared with the global radiation received at the Urdukas AWS since longwave energy fluxes are not measured on-site. Modelled and measured values are in good agreement (R^2 = 0.75). On average, global radiation at the AWS is overestimated by 32.5 W m^{-2}, but higher discrepancies are noticeable during summer (see fig. 2).

Precipitation varies essentially across the Karakoram and follows a clear seasonal cycle. Accumulation takes place mainly between January and April. The corrected and interpolated HAR dataset yields a region-wide mean total precipitation of 520 mm for 2011. Dry valley basins gaining less than 100 mm precipitation per year contrast the humid alpine environment of the central Karakoram with snow accumulation of >1.7 m w.e. a^{-1}. A quantitative precipitation evaluation is lacking because snowfall during wintertime is not reliably detected at the AWS. The agreement between the precipitation events of the HAR dataset and those detected at the Urdukas and Askole AWS is 61% and 64%, respectively.

Debris Cover and Thickness

Based on the evaluation of the classified Landsat images, supraglacial debris covers 18%, bare ice 36% and snow or firn 46% of the glacier area in the Karakoram. On the Baltoro glacier, the fraction of debris-covered ice is larger due to the extensively debris-covered tongue (debris = 24%, bare ice = 34%, firn and snow = 42%). Heavily debris-covered and almost debris-free glaciers coexist across the entire Karakoram (see fig. 5). In the Shaksgam valley, east of the Baltoro glacier, the region-wide maximum of > 1 m debris (South Skyang Glacier) is found. The average debris thickness in the mountain range is 0.12 m. On the Baltoro glacier, the supra-glacial layer ranges from a few mm (dust) up to 0.45 m (debris), with a mean thickness of 0.13 m. While the debris thickness patterns derived from Eqn 4 and Eqn 7 are similar, the empirical approach (Eqn 4) yields higher debris thickness values of up to 1.9 m at the front of the Baltoro glacier. The energy-balance model (Eqn 7) on the contrary better captures debris thickness at higher elevations.

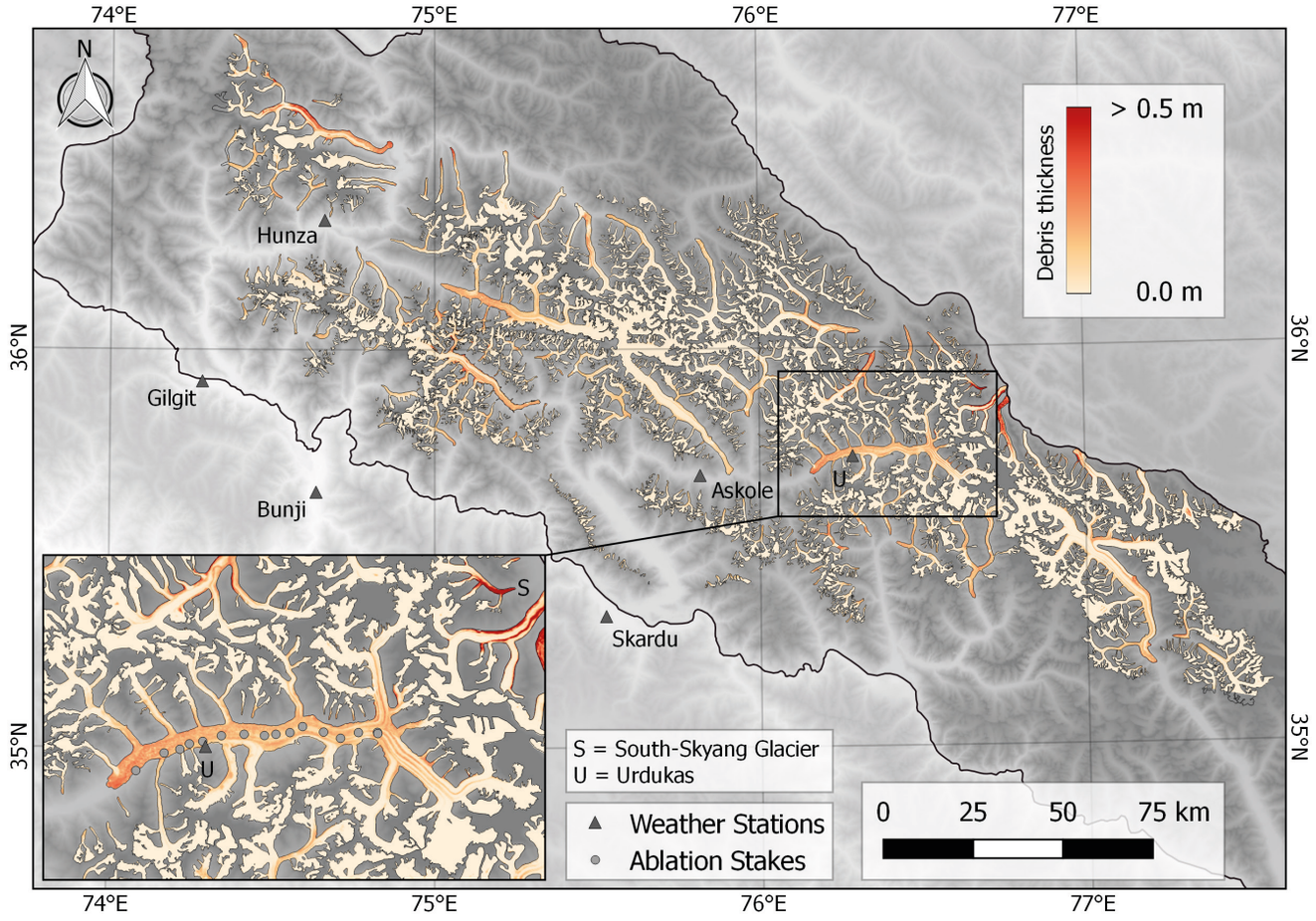

FIG. 5 - Spatial distribution of debris thickness in the Karakoram calculated from land surface temperatures using the energy-balance model described in Eqn 7. The locations of in-situ debris measurements on the Baltoro glacier are displayed in the lower left box.

TABLE 6 - Variables and parameters used in Eqn (11-16) to calculate sub-debris ice melt. The data sources are: 1 = High Asia Refined Analysis dataset (Maussion & *alii*, 2014), 2 = present study, 3 = Conway & Rasmussen (2000), 4 = values taken from Evatt & *alii* (2015) and Nicholson & Benn (2006). The last seven paramters are non-site specific values.

Name	Description	Value	Unit	Reference
NR^+	net radiation	variable	W m^{-2}	1, 2
T^+	air temperature	variable	°C	1, 2
D_T	debris thickness	variable	m	2
k	thermal conductivity	1.3	W m^{-1} K^{-1}	2, 3
q_h	saturated humidity level	variable	kg m^{-3}	2
q_m	measured humidity level	$0.6q_h$	kg m^{-3}	2
ρ_a	air densitiy	variable	kg m^{-3}	2
u_m	wind speed	1.8	m s^{-1}	2
x_m	measurement height	2	m	2
x_r	surface roughness height	0.01	m	4
u_*	friction velocity	0.16	m s^{-1}	4
u_r	slip velocity	=u*	m s^{-1}	4
Φ	volume fraction of debris in ice	0.01	-	4
ν	windspeed attenuation constant	235	-	4
c_a	specific heat capacity of air	1000	J kg^{-1} K^{-1}	4
L_m	latent heat of melting ice	3.34 x 10^5	J kg^{-1}	4
L_v	latent heat of evaporation	2.5 x 10^6	J kg^{-1}	4
$T_{freezing}$	water freezing temperature	273.15	K	4
ε	thermal emissivity	0.95	-	4
ρ_i	ice density	900	kg m^{-3}	4
σ	Stefan-Boltzmann constant	5.67 x 10^{-8}	$W\ m^{-2}\ K^{-4}$	4

TABLE 7 - Output of the glacier surface mass balance model applied for the Baltoro region and entire Karakoram from August 2010 until July 2011. Acc = accumulation, Abl = ablation, M_{DF} = debris-free ice melt, M_{SD} = sub-debris ice melt, M_F = firn melt, M_S = snowmelt, MB = mass balance, ELA = equilibrium line altitude, AAR = accumulation area ratio.

	Acc [m]	Abl [m]	M_{DF} [%]	M_{SD} [%]	M_F [%]	M_S [%]	MB [m]	ELA [m]	AAR
Baltoro	0.86	1.04	44.4	23.4	6.0	26.2	-0.18	5,145	0.50
Karakoram	0.79	1.71	55.7	18.9	6.6	18.9	-0.92	5,145	0.43

Glacier Surface Mass Balance

During the evaluation period from 1st August 2010 until 31st July 2011, modelled ablation and accumulation on the Baltoro glacier varies considerably in space (see fig. 6) and time (see fig. 7). Ablation occurs mainly between April and September, whereas accumulation takes place mostly between January and May. Maximum snow deposits on the Baltoro glacier exceeding 1.5 m w.e. are found in the upper accumulation areas. Glacier mass loss across the ablation zone depends on the surface cover. Ice melt rates of up to 8 m w.e. a^{-1} are characteristic of the lower and almost debris-free parts of the tributary glaciers. In contrast, sub-debris ice melt close to the heavily debris-covered snout is reduced to less than 1.2 m w.e. a^{-1}. The difference between the mean annual accumulation (0.86 m w.e. a^{-1}) and ablation (1.04 m a^{-1}) results in a slightly negative surface mass balance for the Baltoro glacier of -0.18 m w.e. a^{-1} (see tab. 7). This corresponds to a fresh water storage in winter of 0.54 km^3 and a melt water release in summer of 0.66 km^3. A good agreement between the modelled surface mass balance above the Concordia profile and the estimated long-term mean ice volume flow at the profile (0.1207 vs. 0.1164 km^3) confirms that the dominant accumulation and ablation processes can, at least for the Baltoro region, be reproduced with glacierSMBM. Although the temporal evolution of mass gain and loss in the Karakoram follows the same pattern as outlined before, the modelled region-wide glacier surface mass balances vary across the mountain range and are on average more negative (-0.92 m w.e. a^{-1},

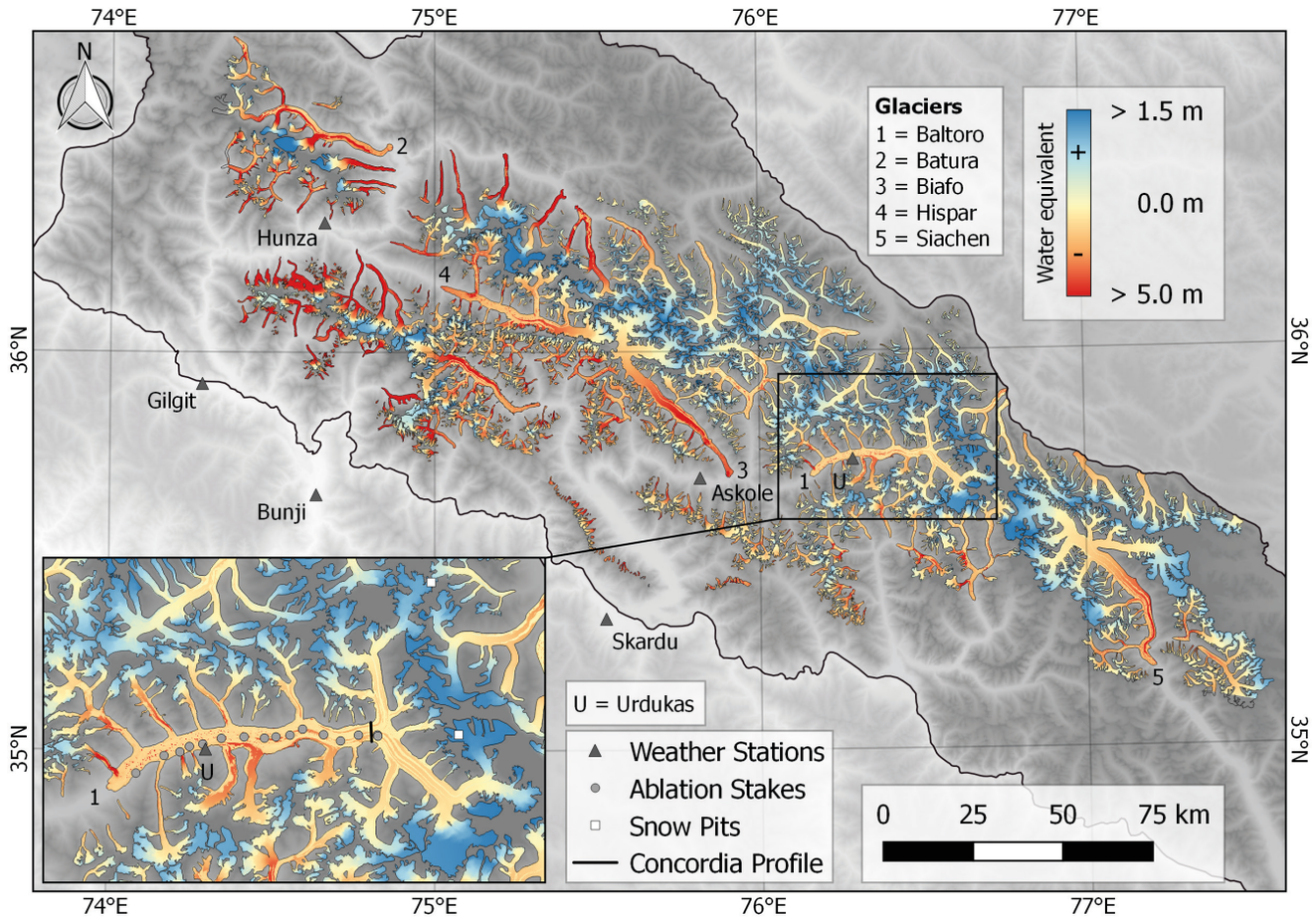

FIG. 6 - Modelled surface mass balances from 1st August 2010 until 31st July 2011 for all Karakoram glaciers included in the inventory. The spatial mass balance pattern of the Baltoro glacier is highlighted in more detail in the lower left box.

see tab. 7). Glaciers with stable or positive annual mass balances are located, with only few exceptions, in the central and northeastern Karakoram, whereas negative mass balances are typical for the southern and western part (see fig. 8). Most glaciers with a distinct negative mass balance (-2 to -8 m a^{-1} w.e.) are relatively small in size (0.25 - <15 km^2), are on average located below 5,500 m a.s.l., advance in some cases down to elevations of <2,500 m (a.s.l.) and have a low AAR (<0.2). While glaciers with a mean elevation above 5,500 m a.s.l. have on average a positive modelled surface mass balance (0.62 m w.e.), the mass balance of those below is clearly negative (-1.43 m w.e.). At altitudes, where the annual mean air temperature is about 10 °C, modelled ice melt rates of up to 15 m w.e. a^{-1} can be reached in the western Karakoram. The highest accumulation rates of up to 1.7 m w.e. a^{-1} are found between 6,000 and 7,000 m a.s.l. in the central Karakoram. During the whole modelling period, snow in the order of 5.89 km^3 (w.e.) is accumulated over the glaciated area in the Karakoram, while the glacial melt water contribution during the ablation season is 12.66 km^3. The number of ablation and accumulation days is similar (196 vs. 227).

Transitional snow line altitudes

Transitional snow line altitudes (TSLAs) derived from the MODIS Snow Cover Product for the entire Karakoram follow a clear seasonal cycle (see Fig. 9). Between November and March, the TSLA reaches its minimum and falls below 3,700 m (a.s.l.). From then on, it rises steadily and reaches a maximum elevation of 5,400 ± 200 m at the end of August. The seasonal cycle and timing of the highest annual TSLAs can be reproduced with the model, but this does not hold true for the onset of the supraglacial snow melt as well as the downward propagation of the snow cover after the ablation season. The modelled beginning of snowmelt lags several weeks behind the observed onset.

Sensitivity Analysis

Modified meteorological and glaciological conditions affect the modelled surface mass balance of the Baltoro glacier in various ways (see tab. 8). Snow accumulation in the upper parts of the glacier is obviously linked to changes in precipitation. A 10% increase or decrease of solid pre-

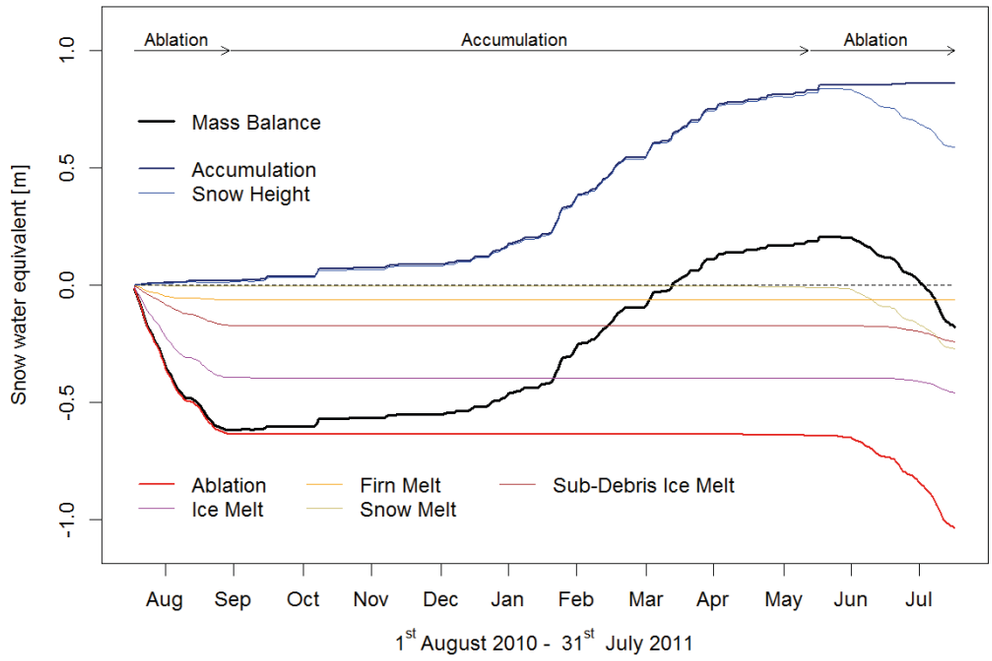

FIG. 7 - Temporal evolution of the modelled mean surface mass balance of the Baltoro glacier in m w.e. from 1st August 2010 until 31st July 2011. An animation showing the modelled temporal and spatial surface mass balance variations of the Baltoro glacier during the study period is available online (Groos & *alii*, 2017).

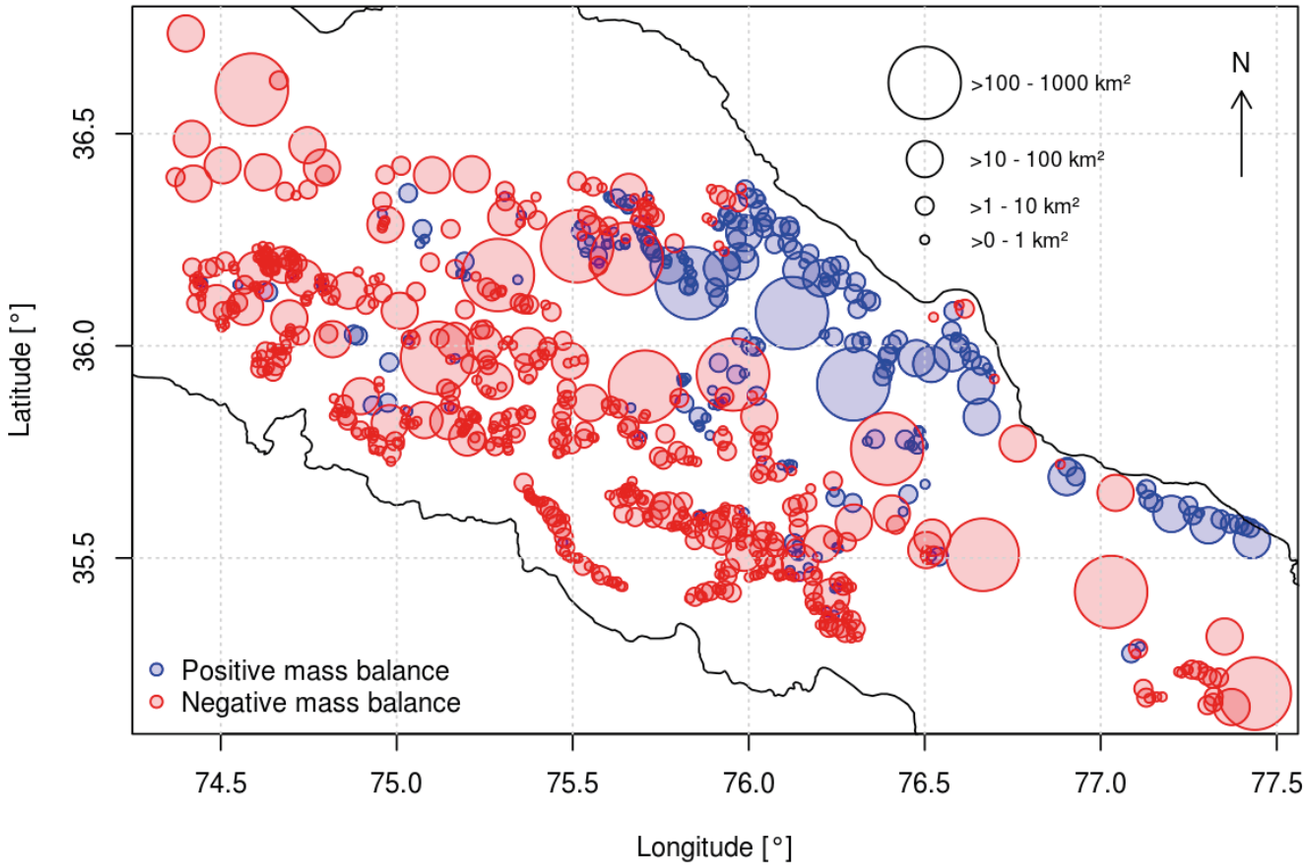

FIG. 8 - Distribution of glaciers in the Karakoram with a modelled positive or negative annual surface mass balance (1st August 2010 - 31st July 2011). The area (in km²) of the glaciers is indicated by the size of the circles.

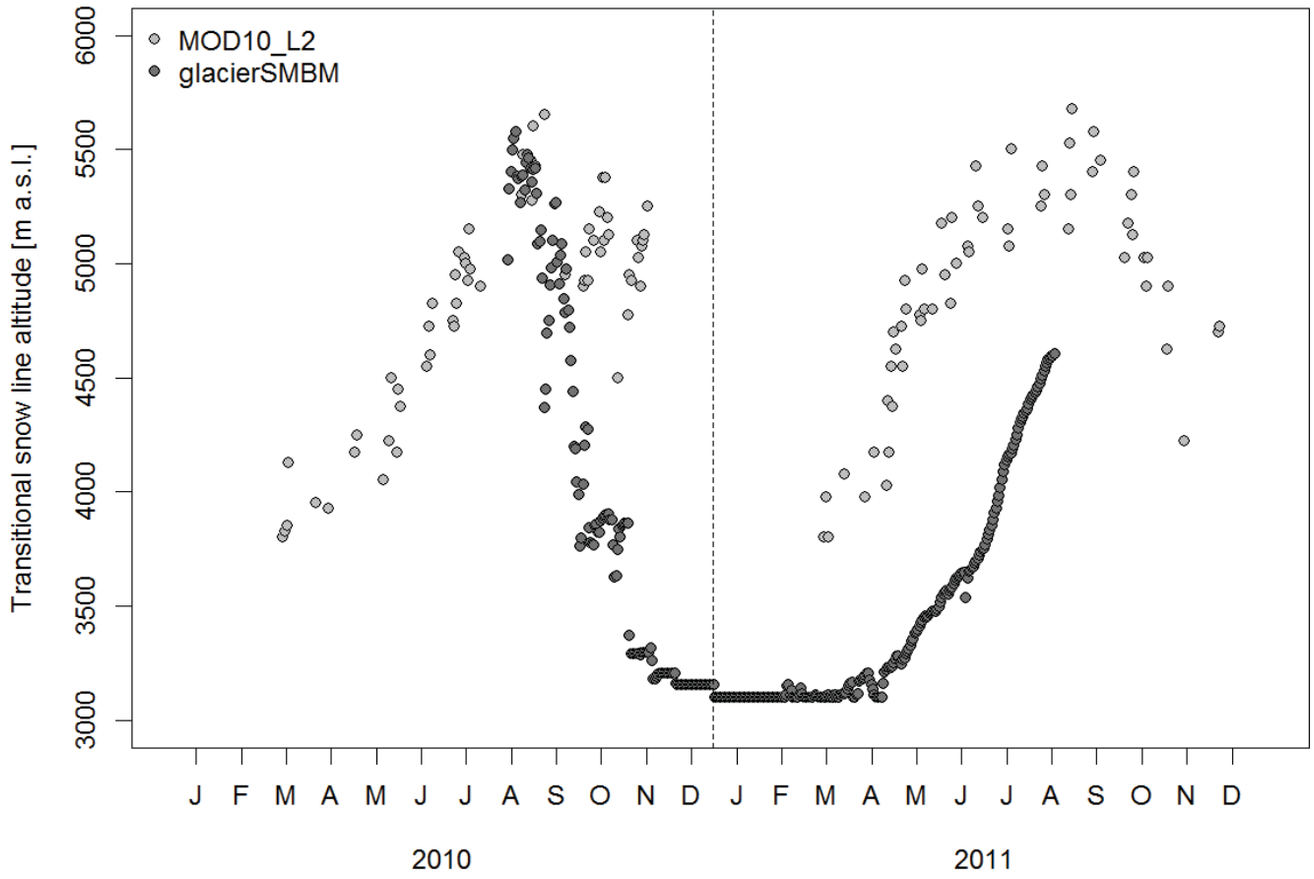

FIG. 9 - Temporal evolution of the transitional snow line altitude in the Karakoram during 2010 and 2011 derived from the MODIS Snow Cover Product (MOD10_L2) and the daily model output (glacierSMBM).

cipitation results in a mean accumulation change of plus and minus 10%, respectively. Stronger changes are observed when an intensified monsoonal influence, simulated by a six-month precipitation shift towards a culmination during the ablation season, is assumed. In this case, the glacier-wide accumulation is reduced by 23%. Even though snowfall in glacierSMBM is defined as precipitation at temperatures ≤1 °C (Eqn 9), modifications of air temperature have almost no effect on the amount of accumulation. However, when precipitation is shifted in time and the main snowfall events coincide with the ablation period, it reacts very sensitive to rising temperature, leading to a mean accumulation decrease of 30%.

Air temperature and debris thickness are the dominant controls on ablation on the Baltoro glacier. A temperature increase of 2 K yields on average a 44% higher ablation, while a decrease of 2 K leads to a drop of 35%. The strong relationship as well as the minor impact of changes in net radiation are attributed to the setup of the enhanced degree-day model with air temperature as main predictor for snow and ice melt (Eqn 10). In contrast to snow and debris-free ice, debris-covered ice reacts more sensitively to variations in net radiation. Based on the sensitivity test where debris was excluded, the debris layer on the Baltoro glacier reduces ablation by ~35%. Similar results are obtained when the empirically derived debris thickness distribution serves as an input dataset. A doubling of the debris thickness has a weaker impact due to the exponential decrease of melt rates with increasing thickness (see fig. 4). Besides air temperature, net radiation and debris thickness, the often-unknown thermal properties of the debris layer have a noticeable effect on the sub-debris ice melt.

The modelled surface mass balance of the Baltoro glacier responds most sensitively to variations in air temperature, the absence of supra-glacial debris and the shift of precipitation towards a maximum during the main ablation season. In consequence, climatic conditions (a monsoonal precipitation regime in combination with increasing air temperatures) as observed in the central and eastern Himalaya (e.g. Kapnick & *alii*, 2014) would lower the ELA and decrease the AAR considerably, resulting in a pronounced negative mass balance of -0.91 m w.e. a^{-1}.

TABLE 8 - Sensitivity tests performed by using modified meteorological and glaciological data as input for glacierSBMB. $Precip_{\pm 10\%}$ = precipitation increase/decrease of 10 %, $Precip_{shift}$ = precipitation input shifted by 6 months, $T2m_{\pm 2K}$ = air temperature increase/decrease of 2 K, $NetRad_{\pm 20W}$ = net radiation increase/decrease of 20 W, $TMF_{\pm 10\%}$ = increase/decrease of the temperature melting factors by 10%, $RMF_{\pm 10\%}$ = increase/decrease of the radiative melting factors by 10%, $DT_{empirical}$ = empirically derived debris thickness (Eqn 4), $DT_{+100\%}$ = debris thickness doubled, $DT_{-100\%}$ = no debris cover considered, $k_{1.8}$ = thermal conductivity of the debris layer increased by 0.5 W m^{-1} K^{-1}, $k_{0.8}$ = thermal conductivity of the debris layer decreased by 0.5 W m^{-1} K^{-1}, $Precip_{shift}$ & $T2m_{+2K}$ = precipitation shifted by 6 months while air temperature is increased by 2K. The three most influential parameters on the mass balance variables are underlined.

	Acc [Δm]	Abl [Δm]	M_{DF} [Δm]	M_{SD} [Δm]	M_F [Δm]	M_S [Δm]	MB [Δm]	ELA [Δm]	AAR [Δ]
Reference	0.86	1.04	0.46	0.24	0.06	0.27	-0.18	5,145	0.50
$Precip_{+10\%}$	0.09	0.00	-0.01	0.00	0.00	0.02	0.08	-10	0.02
$Precip_{-10\%}$	-0.09	0.00	0.01	0.01	0.00	-0.01	-0.08	40	-0.02
$Precip_{shift}$	-0.20	-0.02	0.04	0.03	-0.01	-0.07	-0.18	100	-0.05
$T2m_{+2K}$	-0.01	0.46	0.25	0.06	0.08	0,1	-0.49	170	-0.12
$T2m_{-2K}$	0.00	-0.36	-0.18	-0.04	-0.04	-0.09	0.36	-160	0.11
$NetRad_{+20W}$	0.00	0.07	0.02	0.05	0.01	0.01	-0.08	30	-0.01
$NetRad_{-20W}$	0.00	-0.07	-0.02	-0.04	0.00	-0.01	0.07	-10	0.01
$TMF_{+10\%}$	0.00	0.06	0.05	0.01	0.01	0.01	-0.06	30	-0.01
$TMF_{-10\%}$	0.00	-0.06	-0.04	0.00	0.00	-0.01	0.06	-10	0.01
$RMF_{+10\%}$	0.00	0.01	0.01	0.00	0.00	0.01	-0.02	0	-0.01
$RMF_{-10\%}$	0.00	-0.01	-0.01	0.00	0.00	0.00	0.02	0	0.00
$DT_{empirical}$	0.00	0.02	0.00	0.03	0.00	0.00	-0.03	0	0.00
$DT_{+100\%}$	0.00	-0.08	0.00	-0.07	0.00	0.00	0.08	0	0.00
$DT_{-100\%}$	0.00	0.57	0.82	-0.24	0.00	0.00	-0.57	0	-0.01
$k_{0.8}$	0.00	-0.06	0.00	-0.05	0.00	0.00	0.05	0	0.00
$k_{1.8}$	0.00	0.04	0.00	0.04	0.00	0.00	-0.04	0	0.00
$Precip_{shift}$&$T2m_{+2K}$	-0.26	0.47	0.34	0.09	0.07	-0.02	-0.73	335	-0.17

DISCUSSION

Glacier Surface Mass Balance

The introduced glacier Surface Mass Balance Model (glacierSMBM) delivers plausible accumulation and ablation results for the Baltoro glacier in the central Karakoram during the observation period from August 2010 until July 2011. Maximum annual melt rates of 7-8 m w.e. a^{-1} at the tongue of the debris-free tributaries of the glacier are in the same order as independent ablation measurements from the Biafo (5-7 m w.e. a^{-1}) and Baturo glacier (~9 m w.e. a^{-1}) (Hewitt & *alii*, 1989). Modelled snow deposits of up to 1.5 w.e. a^{-1} fall in the range of published accumulation values (~1-2 m w.e. a^{-1}) from different areas of the Karakoram (Hewitt & *alii*, 1989; Winiger & *alii*, 2005; Mayer & *alii*, 2014). The agreement between the modelled seasonal evolution of the glacier mass balance (fig. 7) and the meteorological and glaciological observations (dominating winter precipitation and strong melting during August and September) indicate that the model captures the most relevant accumulation and ablation processes of the Baltoro glacier. However, this does not hold true for avalanche-fed glaciers of the so-called Turkestan-Type (Hewitt, 2011), which are characterised by area-wide negative mass balances in the model output and are lacking an "accumulation zone" as normally understood. The imbalance between mass gain and mass loss probably stems from to the lack of snow redistribution.

Compared to the Baltoro glacier, the modelled surface mass balance for the Karakoram under average meteorological conditions (see section *Meteorology*) is more negative (-0.92 m w.e. a^{-1}) and does not match the region-wide averages (-0.10 to + 0.11 m w.e. a^{-1}) derived from satellite-based geodetic measurements (e.g. Gardelle & *alii*, 2012; Kääb & *alii*, 2015). Albeit these studies cover multi-annual observation periods and focus on different regions of the mountain range, the large offset hints that accumulation in the Karakoram might be underestimated and ablation close to the glacier snout overestimated. Despite these absolute differences, the model is able to reproduce the general pattern of the Karakoram Anomaly. Stable or positive mass balances are found in the central and northeastern part of the mountain range and contrast the widespread mass loss in the southern and western valleys (see fig. 8). Evidence from other studies also suggest that the Karakoram is located at the southwestern edge rather than in the centre of the mass balance anomaly, stretching from the western Kunlun Shan

towards the Pamir (Gardelle & *alii*, 2012, 2013; Kääb & *alii*, 2015; Lin & *alii*, 2017). Region-wide geodetic measurements between 1973/74 and 2000 reveal a zonal trend of decreasing negative mass balances from west to east (Zhou & *alii*, 2017). Besides the geographical location, the modelled mass balances are mainly influenced by the size and elevation-coverage of the glaciers. Out of all glaciers with a pronounced modelled negative mass balance (-2 – -8 m w.e.), 50% are smaller than 6 km^2 and 100% are on average located below 5,500 m (a.s.l.). Findings by Qureshi & *alii* (2017) reveal a similar pattern. The authors used different satellite products to examine glacier changes in the Hunza basin (western Karakoram) and found out that extensive area loss is especially characteristic for glaciers small in size or located below (5,500 m a.s.l.). Glaciers of less than a few km^2 respond very sensitively to rising temperatures, as a recent study from the European Alps emphasizes (Huss & Fischer, 2016). In the Karakoram, small glaciers have experienced little scientific attention, albeit they might contradict the postulated general mass balance anomaly in the region.

By evaluating the results of the sensitivity analysis, two characteristic glaciological and climatological features promoting stable mass balances in the Karakoram become apparent:

Extensive and thick debris (> 4-5 cm) reduces the annual ice melt rate by ~35% and contributes to the conservation of glacier ice in the lower ablation zone. A similar mass-conserving effect due to the isolating character of debris was found by Collier & *alii* (2015) and Minora & *alii* (2015). The magnitude of the average ice melt rate across the debris-covered ablation zone might be slightly underestimated in glacierSMBM since the observed amplifying effects of supraglacial lakes and ice cliffs on glacial melt (e.g. Sakai, 2000, 2002; Tedesco & *alii*, 2012; Juen & *alii*, 2014; Brun & *alii*, 2016) are not considered. Based on the investigation of selected ice cliffs on the Lirung glacier in the Nepalese Himalaya, Brun & *alii* (2016) conclude that the mass loss of exposed ice cliffs can be six times higher than the average melt rate across the debris-covered ablation zone. However, since ice cliffs only occupy small areas (e.g. ~1-2%) of debris-covered glaciers and contribute marginally (e.g. ~2.5%) to the total annual ablation (Juen & *alii*, 2014), it seems unlikely that the enhanced melting of ice cliffs equals the mass conserving effect of thick and isolating debris as hypothesised by Gardelle & *alii* (2012).

Snowfall accumulated mainly during winter and spring as observed on the Baltoro glacier (see fig. 7) and in the Karakoram in general responds less sensitively to rising temperatures than snow falling in summer (see tab. 8). An average increase of air temperature by +2K has almost no effect on the modelled annual accumulation of the Baltoro glacier, whereas in a monsoonal precipitation regime the same warming leads to a reduction in snowfall of ~30%. These findings support the conclusion of Kapnick & *alii* (2014) that the characteristic seasonal cycle with dominating winter precipitation is – besides decreasing summer temperatures and increasing winter precipitation (e.g. Archer & Fowler, 2004; Fowler & Archer, 2006; Bocciola & Diolaiuti, 2013) – one of the main meteorological drivers of the Karakoram Anomaly. Fowler & Archer (2006) discuss increasing cloud cover as a potential cause for the observed decreasing summer temperatures. Furthermore, they point out that warming may occur predominantly in higher elevations (> 2,500 m a.s.l.) where almost no long-term AWS-records are available.

The sensitivity analysis not only highlights potential causes for the observed stable mass balance in the Karakoram, but also reveals that the glaciers in the region might respond very sensitively to climatic and glaciological changes; especially to variations in debris thickness, air temperature, radiative forcing, snowfall and the timing of the prevailing precipitation season. Thus, it should be questioned whether the debris-covered glaciers in the Karakoram are as resistant to climatic changes as previously assumed.

Model Limitations and Data Uncertainties

The spatial and temporal interpretation of the modelled region-wide surface mass balances is hampered by the presence of data uncertainties, the lack of observational data for calibration and validation as well as the non-consideration of glaciological processes like snow redistribution or the melt contribution of supraglacial ice cliffs and ponds.

Even though the importance of avalanches for glacier nourishment in the Karakoram has been outlined by Hewitt (2005, 2011), the quantitative mass contribution ascribed to redistributed snow has not been further investigated yet. The modelled area-wide negative mass balance of numerous small glaciers indicate that they could probably not withstand strong melting without the additional mass input from adjacent slopes. Laha & *alii* (2017) evaluated the impact of avalanching on the mass balance of four Himalayan glaciers (area: 2.4 – 19.0 km^2) and calculated that the contribution can account for up to 1.8 m w.e. a^{-1}. For further mass balance studies in HMA, implementing the processes of gravitational mass movement (e.g. Bernhardt & Schulz, 2010) and snow redistribution by wind (e.g. Warscher & *alii*, 2013) is necessary. The consideration of snowmelt induced by short- and longwave radiation at air temperatures below freezing may help to minimise the gap between the observed and modelled onset of ablation. However, the delayed upward-shift of the TSLA could be also ascribed to the negative temperature bias during spring or an overestimation of accumulation in the valley bottoms. Enhanced melting due to exposed ice cliffs and supraglacial ponds may compensate for the effects of thick and isolating debris and has been mentioned as a possible cause that could explain the observed similar area-wide melt rates of debris-free and debris-covered glaciers (Gardelle & *alii*, 2012). To test this hypothesis, a parametrisation of small-scale features across the debris-covered ablation zone is required. Recently developed methods to quantify melt resulting from ice cliffs (Juen & *alii*, 2014; Reid & Brock, 2014; Steiner & *alii*, 2015; Buri & *alii*, 2016; Brun & *alii*, 2016) and meltwater ponds (Tedesco & *alii*, 2012; Juen & *alii*, 2014) should be further explored for this purpose.

In addition to the glaciological processes not being

implemented in the model, uncertainties are introduced by the applied datasets. The original validation of the meteorological HAR dataset focuses rather on the Tibetan Plateau than on the western part of High Mountain Asia (see fig. 1 in Maussion & *alii*, 2014). Therefore, the overall accuracy of the dataset in the Karakoram remains uncertain. The horizontal HAR-resolution of 10 km is much higher than the pixel size of gridded datasets provided from general circulation models, but is still not sufficient to resolve the precipitation, temperature, pressure and radiation distribution in a complex terrain like the Karakoram. Different methods of varying complexity were applied to interpolate the meteorological variables to a spatial resolution of 30 m. While interpolated HAR air temperatures are in good agreement with measurements from the Urdukas and Askole AWS (see fig. 2), there is the need to further improve the accuracy of distributed net radiation and precipitation in the region. This can be achieved either by advanced statistical downscaling or by the use of a physical high-resolution meso-scale atmospheric model that considers the complex topography and incorporates feedbacks from glacier mass balance changes to the atmosphere (Collier & *alii*, 2013).

In addition to the mass contribution of avalanches, topographic shading from steep slopes and cliffs rising more than several hundred meters above the valley floor support the existence of small and medium-size glaciers (e.g. Wagnon & *alii*, 2007; Huss & Fischer, 2016). Shading plays probably a minor role in the wide valleys of the Biafo, Hispar and Baltoro glacier, but it must be assumed that the mass balance of glaciers in the narrow and deeply-incised valleys of the Karakoram is considerably altered by the reduced energy input due to the shielding of incoming short-wave radiation. Hence, short- and longwave downward radiation should be corrected for shading effects and cloudiness in future modelling approaches (e.g. Senese & *alii*, 2016). Gridded precipitation data, which are a prerequisite for the quantification of region-wide snow accumulation, are still prone to significant errors and are not able to reproduce the orographically influenced vertical and lateral variability in the Karakoram (Dahri & *alii*, 2016). With respect to further investigations of the drivers of the Karakoram Anomaly, the development of an accurate, distributed precipitation dataset for the region, along with high-elevation accumulation studies is pressing. Accumulation studies as conducted by Mayer & *alii* (2014) are not only valuable for the understanding of seasonal precipitation patterns and detection of longterm trends, but also for the determination of the thickness of the firn layer. Such information is needed for the projection of long-term glacier changes. In addition to emerging englacial debris, an upward-shift of the ELA is associated with higher melt rates since the underlying ice has a lower albedo than the snow or firn above.

Melting factors for snow and ice obtained from ablation stake readings on the Baltoro glacier are in the same order as those published by Lutz & *alii* (2016) and were – due to the absence of concurrent measurements in other parts of the mountain range – taken as constant in space and time. However, it is likely that the melting factors vary regionally since the amount of melted snow or ice does not only depend on the incoming energy fluxes, but also on further meteorological variables (e.g. relative humdity and windspeed) and the physical properties (e.g. density and albedeo) of ice or snow. High wind speeds and a low relative humidity for example cause a higher saturation deficit and favour sublimation, which in turn consumes more energy and leads to a lower ablation rate than the melting of snow and ice (e.g. Hock, 2003). The variability of wind speed, relative humidity and glacier albedo has so far not been further investigated in the Karakoram. To validate whether the modelled maximum ice melt rates of up to 15 m w.e. a^{-1} at the lowest and debris-free glacier tongues are real or the result of biased melting factors, remains a subject for future ablation studies.

One of the main improvements in glacierSMBM against other mass balance models is the implementation of the non-linear debris effect on sub-surface ice melt. In order to model sub-debris ice melt rates, information on the thickness and properties of the layer are essential. The debris thickness datasets obtained from remotely-sensed land surface temperatures are promising. They deliver plausible values for the Baltoro glacier and capture the spatial debris variability in the Karakoram. A reliable validation would, however, require a denser network of ablation stakes or other spatial information regarding the debris thickness (e.g. from ground-penetrating radar; McCarthy & *alii*, 2017) to account for the sub-pixel variability. More important than the further improvement of the debris thickness datasets seems the investigation of the thermal properties and albedo of the debris layer. Both variables were treated homogeneously across the ablation zone. Lithological units of debris on the Baltoro glacier as identified on satellite imagery by Gibson & *alii* (2016) could help to distribute thermal conductivities depending on the rock type. Glacier-wide surface albedos can be derived from optical satellite data (e.g. Sentinel-2 and Landsat 8) as demonstrated by Neageli & *alii* (2017).

For future mass balance studies, the missing small and medium-size glaciers in the west, north and southeast should be also included in the inventory. They are already available in some inventories (see tab. 1), but the provided outlines incorporate processing artefacts like nunataks and steep ice-free slopes. Plateaus and slopes above the glacier trunks are an important source for avalanches (e.g. Hewitt, 2011), but they do not belong to the accumulation area where glacier ice is formed. Thus, an inventory, which distinguishes between glacier outlines, rock surfaces and potential source regions for avalanches and snowdrift, would be favourable.

CONCLUSION

In this study, we present a new open-source high-resolution glacier Surface Mass Balance Model (glacierSMBM) which takes the non-linear effect of supra-glacial debris on sub-surface ice melt into account. Data from field measurements, remote-sensing observations and climate reanalysis are used as input to test the applicability and limitations of the model in the Karakoram. Accumulation and ablation

rates are calculated at daily timesteps from 1st August 2010 until 31st July 2011 for each glacier in the inventory. For the Baltoro glacier in the central part of the mountain range, where most of the data for the calibration were obtained, the model yields a slightly negative surface mass balance of -0.18 m w.e. a^{-1}. The modelled ablation and accumulation rates are in the order of independent measurements from glaciers nearby and correspond to a fresh water storage during winter of 0.54 km^3 and a melt water release during the ablation season of 0.66 km^3. For the entire Karakoram, the modelled surface mass balance is more negative (-0.92 m w.e. a^{-1}) and associated with an annual melt water contribution of 12.66 km^3. Despite the neglected process of snow redistribution, the model reproduces the characteristic features of the Karakoram Anomaly and emphasises that stable and positive mass balances are rather typical for the central and northeastern part than for the entire mountain range. Results from the sensitivity analysis indicate that the melt-reducing effect of thick debris as well as the timing of the dominant precipitation season are, in addition to the observed decreasing summer temperatures and increasing winter precipitation, important factors promoting stable mass balances in the region. However, since the sensitivity analysis also reveals a distinct mass balance response to variations in air temperature, precipitation, debris thickness etc., the common image of the Karakoram as a mountain range being resistant to recent climate changes should be challenged. For a more sound and detailed regional analysis of the drivers of the Karakoram Anomaly, the modification of the input datasets as well as the implementation of further glaciological processes into glacierSMBM is necessary. Snow redistribution in the accumulation area along with enhanced melting ascribed to small-scale features like exposed ice cliffs and supraglacial melt water ponds across the ablation zone are assumed to be the most relevant processes not considered in the model so far. Regarding the gridded input datasets, increasing the accuracy of precipitation and determining the glacier surface albedo and thermal properties are probably the most urgent objectives. An intensification and expansion of in-situ accumulation and ablation studies on different glaciers in this remote environment is required to allow for a proper calibration and validation of the applied datasets and obtained model results. With the realisation of the outlined modifications, the observation period can be extended to compare the model output with multi-annual geodetic mass balance measurements and to simulate the future response of Karakoram glaciers to recent climate change.

REFERENCES

Agarwal V., Bolch T., Syed T.H., Pieczonka T., Strozzi T. & Nagaich R. (2017) - *Area and mass changes of Siachen Glacier (East Karakoram).* Journal of Glaciology, 63, 148-163.

Archer D.R. & Fowler H.J. (2004) - *Spatial and temporal variations in precipitation in the Upper Indus Basin, global teleconnections and hydrological implications.* Hydrology and Earth System Sciences Discussions, 8, 47-61.

Barsi J.A., Barker J.L. & Schott J.R. (2003) - *An atmospheric correction parameter calculator for a single thermal band earth-sensing instrument.* Geoscience and Remote Sensing Symposium, 2003, 3014-3016.

Barsi J.A., Schott J.R., Palluconi F.D. & Hook S.J. (2005) - *Validation of a web-based atmospheric correction tool for single thermal band instruments.* Proceeding of SPIE 58820E-1.

Barsi J.A., Hook S.J., Schott J.R., Raqueno N.G. & Markham B.L. (2007) - *Landsat-5 Thematic Mapper Thermal Band Calibration Update.* IEEE Geoscience and Remote Sensing Letters, 4, 552-555.

Bernhardt M. & Schulz K. (2010) - *SnowSlide: A simple routine for calculating gravitational snow transport.* Geophysical Research Letters, 37, 1-6.

Bhutiyani M.R. (1999) - *Mass-balance studies on Siachen Glacier in the Nubra valley, Karakoram Himalaya, India.* Journal of Glaciology, 45, 112-118.

Bivand R., Keitt T., Rowlingson B., Pebesma E., Sumner M., Hijmans R. & Rouault E. (2017) - *rgdal: Bindings for the Geospatial Data Abstraction Library.* R Package version 1.2-7. https://cran.r-project.org/package=rgdal.

Bocchiola D. & Diolaiuti G. (2013) - *Recent (1980-2009) evidence of climate change in the upper Karakoram, Pakistan.* Theoretical and Applied Climatology, 13, 611-641.

Bocchiola D., Diolaiuti G., Soncini A., Mihalcea C., D'Agata C., Mayer C., Lambrecht A., Rosso R. & Smiraglia C. (2011) - *Prediction of future hydrological regimes in poorly gauged high altitude basins: the case study of the upper Indus, Pakistan.* Hydrology and Earth System Sciences, 15, 2059-2075.

Bocchiola D. & Soncini A. (2017) - *Pasture Modelling in Mountain Areas: the Case of Italian Alps, and Pakistani Karakoram.* Agricultural Research & Technology: Open Access Journal, 8(3), 1-8.

Bolch T., Pieczonka T. & Benn D.I. (2011) - *Multi-decadal mass loss of glaciers in the Everest area (Nepal Himalaya) derived from stereo imagery.* The Cryosphere, 5, 349-358.

Bolch T., Kulkarni A., Kääb A., Huggel C., Paul F., Cogley J.G., Frey H., Kargel J.S., Fujita K., Scheel M., Bajracharya S. & Stoffel M. (2012) - *The State and Fate of Himalayan Glaciers.* Science, 336, 310-314.

Bolch T., Pieczonka T., Mukherjee K. & Shea J. (2017) - *Brief communication: Glaciers in the Hunza catchment (Karakoram) have been nearly in balance since the 1970s.* The Cryosphere, 11, 531-539.

Bookhagen B. & Burbank D.W. (2010) - *Toward a complete Himalayan hydrological budget: Spatiotemporal distribution of snowmelt and rainfall and their impact on river discharge.* Journal of Geophysical Research, 115, 1-25.

Brun F., Buri P., Miles E.S., Wagnon P., Steiner J., Berthier E., Ragettli S., Kraaijenbrink P., Immerzeel W.W. & Pellicciotti F. (2016) - *Quantifying volume loss from ice cliffs on debris-covered glaciers using high-resolution terrestrial and aerial photogrammetry.* Journal of Glaciology, 62(234), 684-695.

Buri P., Miles E.S., Steiner J.F., Immerzeel W.W., Wagnon P. & Pellicciotti F. (2016) - *A physically based 3-D model of ice cliff evolution over debris-covered glaciers.* Journal of Geophysical Research: Earth Surface, 121, 2471-2493.

Chaturvedi R.K., Kulkarni A., Karyakarte Y., Joshi J. & Bala G. (2014) - *Glacial mass balance changes in the Karakoram and Himalaya based on CMIP5 multi-model climate projections.* Climatic Change, 123, 315-328.

Cogley J.G. (2011) - *Present and future states of Himalaya and Karakoram glaciers.* Annals of Glaciology, 52 (59), 69-73.

Cogley J.G. (2016) - *Glacier shrinkage across High Mountain Asia.* Annals of Glaciology, 57 (71), 41-49.

Coll C., Galve J.M., Sanchez J.M. & Caselles V. (2010) - *Validation of Landsat-7/ETM+ Thermal-Band Calibration and Atmospheric Correction With Ground-Based Measurements*. IEEE Transactions on Geoscience and Remote Sensing, 48, 547-555.

Collier E., Mölg T., Maussion F., Scherer D., Mayer C. & Bush A.B.G. (2013) - *High-resolution interactive modelling of the mountain glacier – atmosphere interface: an application over the Karakoram.* The Cryosphere, 7, 779-795.

Collier E., Maussion F., Nicholson L.I., Mölg T., Immerzeel W.W. & Bush A.B.G. (2015) - *Impact of debris cover on glacier ablation and atmosphere – glacier feedbacks in the Karakoram.* The Cryosphere, 9, 1617-1632.

Copland L., Sylvestre T., Bishop M.P., Shroder J.F., Seong Y.B., Owen L.A., Bush A.B.G. & Kamp U. (2011) - *Expanded and Recently Increased Glacier Surging in the Karakoram.* Arctic, Antarctic, and Alpine Research, 43, 503-516.

Dahri Z.H., Ludwig F., Moors E., Ahmad B., Khan A. & Kabat P. (2016) - *An appraisal of precipitation distribution in the high-altitude catchments of the Indus basin.* Science of The Total Environment, 548-549, 289-306.

Diolaiuti G., Pecci M. & Smiraglia C. (2003) - *Liligo Glacier, Karakoram, Pakistan: a reconstruction of the recent history of a surge-type glacier.* Annals of Glaciology, 36(1), 168-172.

Dyurgerov M.B. & Meier M.F. (1997) - *Mass balance of mountain and subpolar glaciers: A new global assessment for 1961-1990.* Arctic and Alpine Research, 29, 379-391.

Dyurgerov M.B. & Meier M.F. (2005) - *Glaciers and the changing earth system: a 2004 snapshot.* Institute of Arctic and Alpine Research, University of Colorado Boulder.

ESA CCI (2015) - *ESA Glaciers_cci Database and CRDP.* https://glaciers-cci.enveo.at/crdp2/index.html.

Evatt G.W., Abrahams D., Heil M., Mayer C., Kingslake J., Mitchell S.L., Fowler A.C. & Clark C.D. (2015) - *Glacial melt under a porous debris layer.* Journal of Glaciology, 61, 825-836.

Feeney G. & Alam I. (2003) - *New estimates and projections of population growth in Pakistan.* Population and Development Review, 29, 483-492.

Fowler H.J. & Archer D.R. (2006) - *Conflicting signals of climatic change in the Upper Indus Basin.* Journal of Climate, 19, 4276-4293.

Foster L.A., Brock B.W., Cutler M.E.J. & Diotri F. (2012) - *A physically based method for estimating supraglacial debris thickness from thermal band remote-sensing data*. Journal of Glaciology, 58, 677-691.

Gardelle J., Berthier E. & Arnaud Y. (2012) - *Slight mass gain of Karakoram glaciers in the early twenty-first century.* Nature Geoscience, 5(5), 322-325.

Gardelle J., Berthier E., Arnaud Y. & Kääb A. (2013) - *Region-wide glacier mass balances over the Pamir-Karakoram-Himalaya during 1999-2011.* The Cryosphere, 7, 1885-1886.

Gibson M.J., Glasser N.F., Quincey D.J., Rowan A.V. & Irvine-Fynn T.D. (2016) - *Changes in glacier surface cover on Baltoro glacier, Karakoram, north Pakistan, 2001–2012.* Journal of Maps, 13, 100-108.

Groos A.R., Mayer C., Smiraglia C., Diolaiuti G. & Lambrecht A. (2017) - *A first attempt to model region-wide glacier surface mass balances in the Karakoram: findings and future challenges, supplementary material.* PANGAEA, https://doi.pangaea.de/10.1594/PANGAEA.880279.

Hall D.K. & Riggs G.A. (2007) - *Accuracy assessment of the MODIS snow products.* Hydrological Processes, 21, 1534-1547.

Hall D.K., Riggs G.A., Salomonson V.V., DiGirolamo N.E. & Bayr K.J. (2002) - *MODIS snow-cover products*. Remote Sensing of Environment, 83, 181-194.

Hewitt K. (2005) - *The Karakoram Anomaly? Glacier Expansion and the "Elevation Effect", Karakoram Himalaya.* Mountain Research and Development, 25, 332-340.

Hewitt K. (2007) - *Tributary glacier surges: an exceptional concentration at Panmah Glacier, Karakoram Himalaya*. Journal of Glaciology, 53, 181-188.

Hewitt K. (2009) - *Rock avalanches that travel onto glaciers and related developments, Karakoram Himalaya, Inner Asia*. Geomorphology, 103, 66-79.

Hewitt K. (2011) - *Glacier Change, Concentration, and Elevation Effects in the Karakoram Himalaya, Upper Indus Basin.* Mountain Research and Development, 31, 188-200.

Hewitt K., Wake C.P., Young G.J. & David C. (1989) - *Hydrological Investigations at Biafo Glacier, Karakoram Range, Himalaya; An Important Source of Water for the Indus River.* Annals of Glaciology, 13, 103-108.

Hijmans R.J., van Etten J., Cheng J., Mattiuzzi M., Sumner M., Greenberg J.A., Lamigueiro O.P., Bevan A., Racine E.B. & Shortridge A. (2016) - *raster: Geographic Data Analysis and Modeling. R package version 2.5-8.* https://CRAN.R-project.org/package=raster.

Hock R. (1999) - *A distributed temperature-index ice- and snowmelt model including direct potential solar radiation.* Journal of Glaciology, 45, 101-111.

Hock R. (2003) - *Temperature index melt modelling in mountain areas*. Journal of Hydrology, 282, 104-115.

Hock R. (2005) - *Glacier melt: a review of processes and their modelling.* Progress in Physical Geography, 29, 362-391.

Hubbard B. & Glasser N.F. (2005) - *Field techniques in glaciology and glacial geomorphology.* John Wiley & Sons, Chichester, 412 pp.

Huintjes E., Li H., Sauter T., Li Z. & Schneider C. (2010) - *Degree-day modelling of the surface mass balance of Urumqi Glacier No. 1, Tian Shan, China*. The Cryosphere Discussions, 4, 207-232.

Huss M. & Fischer M. (2016) - *Sensitivity of Very Small Glaciers in the Swiss Alps to Future Climate Change*. Frontiers in Earth Sciences, 4(34), 1-17.

Immerzeel W.W., van Beek L.P.H. & Bierkens M.F.P. (2010) - *Climate Change Will Affect the Asian Water Towers.* Science, 328, 1382-1385.

Immerzeel W.W., van Beek L.P.H., Konz M., Shrestha A.B. & Bierkens, M.F.P. (2012) - *Hydrological response to climate change in a glacierized catchment in the Himalayas*. Climatic Change, 110, 721-736.

Iqbal M.A., Penas A., Cano-Ortiz A., Kersebaum K.C., Herrero L. & del Río S. (2016) - *Analysis of recent changes in maximum and minimum temperatures in Pakistan*. Atmospheric Research, 168, 234-249.

Juen M., Mayer C., Lambrecht A., Han H. & Liu S. (2014) - *Impact of varying debris cover thickness on ablation: a case study for Koxkar Glacier in the Tien Shan*. The Cryosphere, 8, 377-386.

Kääb A., Berthier E., Nuth C., Gardelle J. & Arnaud Y. (2012) - *Contrasting patterns of early twenty-first-century glacier mass change in the Himalayas*. Nature, 488, 495-498.

Kääb A., Treichler D., Nuth C. & Berthier E. (2015) - *Brief Communication: Contending estimates of 2003-2008 glacier mass balance over the Pamir-Karakoram-Himalaya.* The Cryosphere, 9, 557-564.

Kapnick S.B., Delworth T.L., Ashfaq M., Malyshev S. & Milly P.C.D. (2014) - *Snowfall less sensitive to warming in Karakoram than in Himalayas due to a unique seasonal cycle.* Nature Geoscience, 7, 834-840.

Kaser G., Grosshauser M. & Marzeion B. (2010) - *Contribution potential of glaciers to water availability in different climate regimes.* Proceedings of the National Academy of Sciences, 107, 20223-20227.

KHATTAK M., BABEL M. & SHARIF M. (2011) - *Hydro-meteorological trends in the upper Indus River basin in Pakistan.* Climate Research, 46, 103-119.

KUMAR P., KOTLARSKI S., MOSELEY C., SIECK K., FREY H., STOFFEL M. & JACOB D. (2015) - *Response of Karakoram-Himalayan glaciers to climate variability and climatic change: A regional climate model assessment*. Geophysical Research Letters, 42, 1818-1825.

LAHA S., KUMARI R., SINGH S., MISHRA A., SHARMA T., BANERJEE A., NAINWAL H.C. & SHANKAR R. (2017) - *Evaluating the contribution of avalanching to the mass balance of Himalayan glaciers.* Annals of Glaciology, 1-9.

LIN H., LI G., CUO L., HOOPER A. & YE Q. (2017) - *A decreasing glacier mass balance gradient from the edge of the Upper Tarim Basin to the Karakoram during 2000-2014.* Nature Scientific Reports, 7(1), 1-9.

LUTZ A.F., IMMERZEEL W.W., SHRESTHA A.B. & BIERKENS M.F.P. (2014) - *Consistent increase in High Asia's runoff due to increasing glacier melt and precipitation.* Nature Climate Change, 4, 587-592.

LUTZ A.F., IMMERZEEL W.W., KRAAIJENBRINK P.D.A., SHRESTHA A.B. & BIERKENS M.F.P. (2016) - *Climate Change Impacts on the Upper Indus Hydrology: Sources, Shifts and Extremes*. PLOS ONE, 11, 1-33.

MASON K. (1938) - *Karakoram Nomenclature*. The Himalayan Journal, 10.

MAUSSION F., SCHERER D., MÖLG T., COLLIER E., CURIO J. & FINKELNBURG R. (2014) - *Precipitation Seasonality and Variability over the Tibetan Plateau as Resolved by the High Asia Reanalysis*. Journal of Climate, 27, 1910-1927.

MAYER C., LAMBRECHT A., BELÒ M., SMIRAGLIA C. & DIOLAIUTI G. (2006) - *Glaciological characteristics of the ablation zone of Baltoro glacier, Karakoram, Pakistan*. Annals of Glaciology, 43, 123-131.

MAYER C., LAMBRECHT A., MIHALCEA C., BELÒ M., DIOLAIUTI G., SMIRAGLIA C. & BASHIR F. (2010) - *Analysis of Glacial Meltwater in Bagrot Valley, Karakoram.* Mountain Research and Development, 30, 169-177.

MAYER C., FOWLER A.C., LAMBRECHT A. & SCHARRER K. (2011) - *A surge of North Gasherbrum Glacier, Karakoram, China*. Journal of Glaciology, 57, 1-13.

MAYER C., LAMBRECHT A., OERTER H., SCHWIKOWSKI M., VUILLERMOZ E., FRANK N., DIOLAIUTI G. (2014) - *Accumulation studies at a high elevation glacier site in Central Karakoram.* Advances in Meteorology, 2014, 1-12.

MCCARTHY M., PRITCHARD H., WILLIS I. & KING E. (2017) - *Ground-penetrating radar measurements of debris thickness on Lirung Glacier, Nepal.* Journal of Glaciology, 63(239), 543-555.

MIEHE G., WINIGER M., BÖHNER J. & YILI Z. (2001) - *The Climatic Diagram Map of High Asia: Purpose and Concepts (Klimadiagramm-Karte von Hochasien. Konzept und Anwendung).* Erdkunde, 55, 94-97.

MIHALCEA C., MAYER C., DIOLAIUTI G., LAMBRECHT A., SMIRAGLIA C. & TARTARI G. (2006) - *Ice ablation and meteorological conditions on the debris-covered area of Baltoro glacier, Karakoram, Pakistan*. Annals of Glaciology, 43, 292-300.

MIHALCEA C., MAYER C., DIOLAIUTI G., D'AGATA C., SMIRAGLIA C., LAMBRECHT A., VUILLERMOZ E. & TARTARI G. (2008A) - *Spatial distribution of debris thickness and melting from remote-sensing and meteorological data, at debris-covered Baltoro glacier, Karakoram, Pakistan.* Annals of Glaciology, 48, 49-57.

MIHALCEA C., BROCK B.W., DIOLAIUTI G., D'AGATA C., CITTERIO M., KIRKBRIDE M.P., CUTLER M.E.J. & SMIRAGLIA C. (2008B) - *Using ASTER satellite and ground-based surface temperature measurements to derive supraglacial debris cover and thickness patterns on Miage Glacier (Mont Blanc Massif, Italy).* Cold Regions Science and Technology, 52, 341-354.

MINORA U., BOCCHIOLA D., D'AGATA C., MARAGNO D., MAYER C., LAMBRECHT A., MOSCONI B., VUILLERMOZ E., SENESE A., COMPOSTELLA C., SMIRAGLIA C. & DIOLAIUTI G. (2013) - *2001-2010 glacier changes in the Central Karakoram National Park: a contribution to evaluate the magnitude and rate of the "Karakoram anomaly."* The Cryosphere Discussions, 7, 2891-2941.

MINORA U., SENESE A., BOCCHIOLA D., SONCINI A., D'AGATA C., AMBROSINI R., MAYER C., LAMBRECHT A., VUILLERMOZ E., SMIRAGLIA C. & DIOLAIUTI G. (2015) - *A simple model to evaluate ice melt over the ablation area of glaciers in the Central Karakoram National Park, Pakistan*. Annals of Glaciology, 56, 202-216.

MINORA U., BOCCHIOLA D., D'AGATA C., MARAGNO D., MAYER C., LAMBRECHT A., VUILLERMOZ E., SENESE A., COMPOSTELLA C., SMIRAGLIA C. & DIOLAIUTI G. (2016) - *Glacier area stability in the Central Karakoram National Park (Pakistan) in 2001-2010: The "Karakoram Anomaly" in the spotlight*. Progress in Physical Geography, 1-32.

MIRZA U.K., AHMAD N., MAJEED T. & HARIJAN K. (2008) - *Hydropower use in Pakistan: Past, present and future.* Renewable and Sustainable Energy Reviews, 12, 1641-1651.

MUHAMMAD S. & TIAN L. (2016) - *Changes in the ablation zones of glaciers in the western Himalaya and the Karakoram between 1972 and 2015.* Remote Sensing of Environment, 187, 505-512.

NASA (2011) - Landsat 7 Science Data Users Handbook.

NAEGELI K., DAMM A., HUSS M., WULF H., SCHAEPMAN M. & HOELZLE M. (2017) - *Cross Comparison of Albedo Products for Glacier Surfaces Derived from Airborne and Satellite (Sentinel-2 and Landsat 8) Optical Data.* Remote Sensing, 9(110), 1-22.

ØSTREM, G. (1959) - *Ice Melting under a Thin Layer of Moraine, and the Existence of Ice Cores in Moraine Ridges.* Geografiska Annaler, 41, 228-230.

PAUL F. (2015) - *Revealing glacier flow and surge dynamics from animated satellite image sequences: examples from the Karakoram.* The Cryosphere, 9, 2201-2214.

PEBESMA E., BIVAND R., ROWLINGSON B., GOMEZ-RUBIO V., HIJMANS R., SUMNER M., MACQUEEN D., LEMON J. & O'BRIEN J. (2016) - *sp: Classes and Methods for Spatial Data. R Package version 1.2-4.* https://CRAN.R-project.org/package=sp.

PELLICCIOTTI F., BROCK B., STRASSER U., BURLANDO P., FUNK M. & CORRIPIO J. (2005) - *An enhanced temperature-index glacier melt model including the shortwave radiation balance: development and testing for Haut Glacier d'Arolla, Switzerland.* Journal of Glaciology, 51, 573-587.

PRITCHARD H. (2017) - *Asia's glaciers are a regionally important buffer against drought.* Nature, 545, 169-177.

QUINCEY D.J., GLASSER N.F., COOK S.J. & LUCKMAN A. (2015) - *Heterogeneity in Karakoram glacier surges.* Journal of Geophysical Research: Earth Surface, 120, 1288-1300.

QURESHI A.S., MCCORNICK P.G., SARWAR A. & SHARMA B.R. (2010) - *Challenges and Prospects of Sustainable Groundwater Management in the Indus Basin, Pakistan.* Water Resources Management, 24, 1551-1569.

QURESHI M.A., YI C., XU X. & LI Y. (2017) - *Glacier status during the period 1973-2014 in the Hunza Basin, Western Karakoram.* Quaternary International, 444, 125-136.

RABUS B., EINEDER M., ROTH A. & BAMLER R. (2003) - *The shuttle radar topography mission – a new class of digital elevation models acquired by spaceborne radar.* Journal of Photogrammetry and Remote Sensing, 57 (4), 241-262.

RANKL M. & BRAUN M. (2016) - *Glacier elevation and mass changes over the central Karakoram region estimated from TanDEM-X and SRTM/X-SAR digital elevation models.* Annals of Glaciology, 51 (71), 273-281.

RANKL M., KIENHOLZ C. & BRAUN M. (2014) - *Glacier changes in the Karakoram region mapped by multimission satellite imagery.* The Cryosphere, 8, 977-989.

R Development Core Team (2017) - *R: A language and environment for statistical computing.* R Foundation for Statistical Computing, Vienna, Austria. URL http://www.R-project.org/.

Reid T.D & Brock B.W. (2010) - *An energy-balance model for debris-covered glaciers including heat conduction through the debris layer.* Journal of Glaciology, 56, 903-916.

Reid T.D & Brock B.W. (2014) - *Assessing ice-cliff backwasting and its contribution to total ablation of debris-covered Miage glacier, Mont Blanc massif, Italy.* Journal of Glaciology, 60, 6-13.

Rohrer M. & Braun L. (1994) - *Long-Term Records of Snow Cover Water Equivalent in the Swiss Alps 2. Simulation.* Nordic Hydrology, 25, 65-78.

Rounce D.R. & McKinney D.C. (2014) - *Debris thickness of glaciers in the Everest area (Nepal Himalaya) derived from satellite imagery using a nonlinear energy balance model.* The Cryosphere, 8, 1317-1329.

Round V., Leinss S., Huss M., Haemmig C. & Hajnsek I. (2016) - *Surge dynamics and lake outbursts of Kyagar Glacier, Karakoram.* The Cryosphere, 11, 723-739.

Sakai A., Takeuchi N., Fujita K. & Nakawo M. (2000) - *Role of supraglacial ponds in the ablation process of a debris-covered glacier in the Nepal Himalayas.* In: Debris covered Glaciers. IAHS Publication No. 265, 119-132.

Sakai A., Nakawo M. & Fujita K. (2002) - *Distribution characteristics and energy balance of ice cliffs on debris-covered glaciers, Nepal Himalaya.* Arctic Antarctic and Alpine Research, 34, 12-19.

Schauwecker S., Rohrer M., Huggel C., Kulkarni A., Ramanathan A., Salzmann N., Stoffel M. & Brock B. (2015) - *Remotely sensed debris thickness mapping of Bara Shigri Glacier, Indian Himalaya.* Journal of Glaciology, 61, 675-688.

Scherler D., Bookhagen B. & Strecker M.R. (2011) - *Spatially variable response of Himalayan glaciers to climate change affected by debris cover.* Nature Geosience, 4, 156-159.

Senese A., Maugeri M., Ferrari S., Confortola G., Socini A., Bocchiola D. & Doilaituti G. (2016) - *Modelling shortwave and longwave downward radiation and air temperature driving ablation at the Forni Glacier (Stelvio National Park Italy).* Geografia Fisica e Dinamica Quaternaria, 39, 89-100.

Soncini A., Bocchiola D., Confortola G., Bianchi A., Rosso R., Mayer C., Lambrecht A., Palazzi E., Smiraglia C. & Diolaiuti G. (2015) - *Future hydrological regimes in the upper Indus basin: a case study from a high altitude glacierized catchment.* Journal of Hydrometeorology, 16, 306-325.

Soncini A., Bocchiola D., Confortola G., Minora U., Vuillermoz E., Salerno F., Viviano G., Shrestha D., Senese A., Smiraglia C. & Diolaiuti G. (2016) - *Future hydrological regimes and glacier cover in the Everest region: The case study of the upper Dudh Koshi basin.* Science of the Total Environment, 565, 1084-1101.

Steiner J.F., Pellicciotti F., Buri, P., Miles E.S., Immerzeel W.W. & Reid T.D. (2015) - *Modelling ice-cliff backwasting on a debris-covered glacier in the Nepalese Himalaya.* Journal of Glaciology, 61(229), 889-907.

Tedesco M., Lüthje M., Steffen K., Steiner N., Fettweis X., Willis I., Bayou N. & Banwell A. (2012) - *Measurement and modeling of ablation of the bottom of supraglacial lakes in western Greenland.* Geophysical Research Letters, 39, 1-5.

United Nations, Department of Economic and Social Affairs, Population Division (2015) - World Population Prospects: The 2015 Revision, Key Findings and Advance Tables. ESA/P/WP.241.

Wada Y., van Beek L.P.H., Viviroli D., Dürr H.H., Weingartner R. & Bierkens M.F.P. (2011) - *Global monthly water stress: 2. Water demand and severity of water stress.* Water Resources Research, 47, 1-17.

Wada Y., Wisser D., Eisner S., Flörke M., Gerten D., Haddeland I., Hanasaki N., Masaki Y., Portmann F.T., Stacke T., Tessler Z. & Schewe J. (2013) - *Multimodel projections and uncertainties of irrigation water demand under climate change.* Geophysical Research Letters, 40, 4626-4632.

Wagnon P., Linda A., Arnaud Y., Kumar R., Sharma P., Vincent C., Pottakkal J.G., Berthier E., Ramanathan A., Hasnain S.I. & Chevallier P. (2007) - *Four years of mass balance on Chhota Shigri Glacier, Himachal Pradesh, India, a new benchmark glacier in the western Himalaya.* Journal of Glaciology, 53(183), 603-611.

Wake C.P. (1989) - *Glaciochemical Investigations as a Tool for Determining the Spatial and Seasonal Variation of Snow Accumulation in the Central Karakoram, Northern Pakistan.* Annals of Glaciology, 13, 279-284.

Wanders N. & Wada Y. (2015) - *Human and climate impacts on the 21st century hydrological drought.* Journal of Hydrology, 526, 208-220.

Warscher M., Strasser U., Kraller G., Marke T. Franz H. & Kunstmann H. (2013) - *Performance of complex snow cover descriptions in a distributed hydrological model system: A case study for the high Alpine terrain of the Berchtesgaden Alps.* Water Resources Research, 49, 2619-2637.

Winiger M., Gumpert M. & Yamout H. (2005) - *Karakorum-Hindukush-western Himalaya: assessing high-altitude water resources.* Hydrological Processes, 19, 2329-2338.

Zhang Y., Liu S. & Ding Y. (2006) - *Observed degree-day factors and their spatial variation on glaciers in western China.* Annals of Glaciology, 43, 301-306.

Zhou Y., Li Z. & Li J. (2017) - *Slight glacier mass loss in the Karakoram region during the 1970s to 2000 revealed by KH-9 images and SRTM DEM.* Journal of Glaciology, 63 (238), 331-342.

(Ms. received September 01, 2017; accepted November 20, 2017)